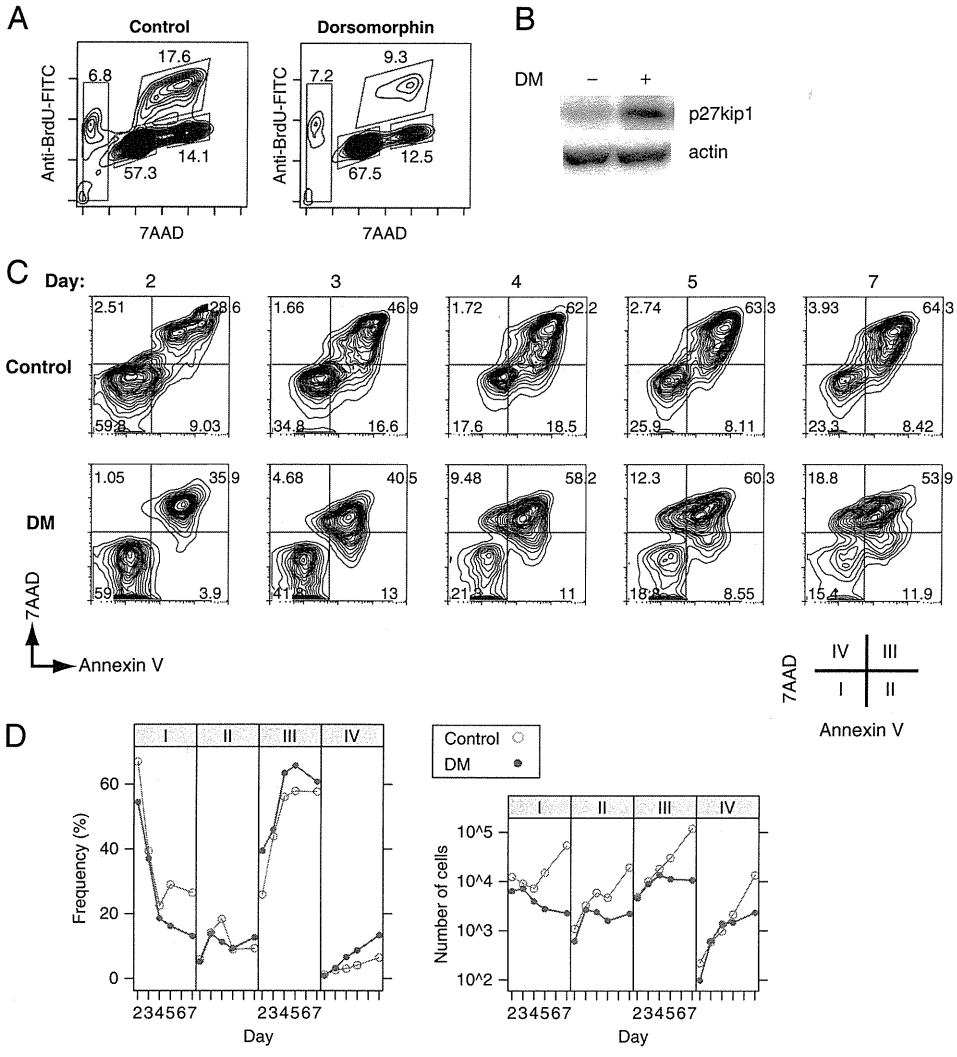

Figure 3. The effects of DM on cell cycle. (A) Jurkat cells were cultured for 2 days with anti-CD3 and -CD28 antibodies with DM (DM, 5 μM) or DMSO as a control, then pulsed with BrdU for last 1 h. Subsequently, cells were fixed, permeabilised, and stained with anti-BrdU and 7AAD. (B) Western blotting analysis of $p27^{kip1}$, cyclin-dependent kinase inhibitor, in DM-treated Jurkat cells. Cells were treated with DM for 30 min, followed by stimulation with anti-CD3 and -CD28 antibodies for 1 h. Actin served as a loading control. (C, D) Analysis of apoptosis in DM-treated T cells by flow cytometry. Freshly isolated $CD4^+CD25^-$ naïve T cells cultured with DM (5 μM), plate bound anti-CD3 and soluble anti-CD28 antibodies for 2–7 days. Cultured cells were fixed and permeabilised, and subsequently stained with AnnexinV and 7AAD. Contour plots in (A) are ungated data. All figures are representative of two independent experiments.

concentrations of DM (0.1–2 μM) in Jurkat cells, and were poorly fit to typical dose–response curves using log-logistic functions in this range, while those at relatively higher concentrations did (Fig. 6A). This wave-like pattern of dose response was also observed in IL-2 production of Jurkat cells cultured with recombinant BMP2 protein (rBMP2, Fig. 6C). Treatment with a fixed concentration of either DM or recombinant Noggin (rNoggin) shifted the multiphasic pattern of IL-2 production by rBMP2 in Jurkat cells (Supporting Information Fig. 4). Treatment with titrated doses of rNoggin showed that there was a significant negative correlation between the dose of rNoggin and IL-2 production ($r = -0.57$, $p<0.001$) by Spearman's correlation coefficient (Fig. 6C). In addition, we have confirmed that knock down of SMAD1 and SMAD5 reduced BMP2-mediated IL-2 production (Fig. 6D). On the other hand, mouse $CD4^+$ T cells were less responsive to rBMP2 and rNoggin, and the correlations between the doses of rNoggin or rBMP2 and IL-2 production were not statistically significant (Fig. 6C). Yet, they showed similar trends to those of Jurkat cells (Fig. 6C). Considering that mouse $CD4^+$ T cells were sensitive to DM in terms of IL-2 production, these results suggest a possibility that the BMP milieu of mouse $CD4^+$ T cells was functionally saturated by a number of BMP ligands. These results collectively suggest that BMP-SMAD signalling regulates *IL2* transcription. The multiphasic effects of DM and rBMP2 suggest that a complex feedback mechanism may exist in BMP-SMAD signalling. Further studies are required to address this point.

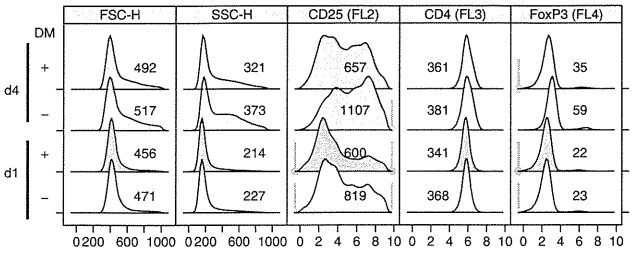

Figure 4. Expression of T-cell activation marker CD25 in DM-treated T cells upon TCR stimulation. Freshly isolated $CD4^+CD25^-$ naïve T cells were cultured with CD3 and -CD28 antibodies with DM (5 μM) or DMSO as a control. Cultured cells were stained with CD25-PE and analysed by flow cytometry on days 1 and 4. These density plots are ungated data. Numbers indicate MFI. Representative results of two independent experiments are shown.

Regulation of phosphorylation of AML1/ RUNX1 by BMP signaling

The results above suggest that BMP signalling modulates RUNX1-mediated *IL2* transcription. As AML/RUNX proteins are reported to be involved in BMP signalling in other tissues such as hematopoitic stem cells [8] and RUNX1 is reported as an important transcription factor for T-cell function including IL-2 production [15], we investigated the molecular mechanism of BMP signalling by analysing RUNX1. The phosphorylated form of RUNX1 with phosphorylation sites including Ser249 is believed to be the activated form of the transcription factor [16]. Thus, we analysed the activity of RUNX1 by flow cytometric analysis with an anti-phospho RUNX1 (pRUNX1, pS249) antibody.

Knock down of RUNX1 in Jurkat cells decreased the staining of both anti-total RUNX1 and anti- pRUNX1 (Fig. 7A), whereas DM decreased only the staining of anti- pRUNX1 (Fig. 7B and 7C). Time course analysis of pRUNX1 showed that BMP2 increased pRUNX1, while DM suppressed pRUNX1 in stimulated Jurkat cells throughout the experiment (Fig. 7D). Given that RUNX1 activates *IL2* transcription [8] and that pRUNX1 is increased by the activation of RUNX1 [16], these results suggested that BMP signalling regulated IL-2 transcription via activating RUNX1 in T cells.

Discussion

This study provides evidence for the multiple roles of BMP signalling in T-cell activation including IL-2 production, proliferation, and T-cell differentiation. In this paper, some of the evidence was obtained by a small molecule inhibitor of the BMP-SMAD signalling pathway, DM. Therefore, we cannot exclude the possibility that DM directly affects other kinases to achieve the observed effects. However, many effects of DM are related to the reported effects of BMP or other related genes. First, DM inhibited known targets of BMP signalling including SMAD1/5/8. Second, DM suppressed the transcription of *IL2*, a RUNX1-target gene [15]. Consistently, we have found that BMP signalling increased the level of phorsphorylation of RUNX1 protein, while DM decreased it. Moreover, both DM and the extracellular BMP antagonist Noggin inhibited IL-2 production by Jurkat cells, demonstrating that the influence of DM on *IL2* transcription is by inhibition of endogenous BMP signalling. Third, DM suppressed proliferation of T cells. In fact, previous reports have suggested that BMPs regulate T-cell proliferation. BMP4 and BMP6 have been reported to increase proliferation, while BMP2 decreased proliferation [17, 18]. Considering the diversity of BMP ligands and receptors, DM may have a profound effect on T-cell proliferation by inhibiting BMP signal transduction via a wide range of BMP ligands and receptors.

DM differentially affected Th differentiation, relatively unaffecting or even augmenting Th2 differentiation, while suppressing Th17 and iTreg cell differentiation, especially in the early phase of the culture, when DM is thought to have the maximal activity in vitro. Although the differentiation of IFN-γ producing cells in the Th1 conditions was more obviously suppressed by DM in the later phase (d4 and 8) of the culture, the decrease of *Tbx21* by DM at 12 h after stimulation suggests that Th1 differentiation is in fact affected. These results collectively indicate that the effects of DM are not simply the results of the inhibition of all TCR signalling and/or the suppression of the expression of the lineage-specific transcription factors. Rather, it is more likely that DM differentially affects multiple mechanisms in T-cell activation and differentiation.

The suppression of proliferation and differentiation by DM was very remarkable at higher doses ($IC_{50} \sim 5$ μM). However, the doses are above IC_{50} of DM on AMP activated kinase and vascular endothelial growth factor kinase [19], although it is not known whether these kinases have significant roles in T cells. Besides, recombinant Noggin did not have remarkable effects in suppressing proliferation and differentiation (data not shown). Therefore, we do not exclude the possibility that the inhibition of proliferation and differentiation was due to disturbing not only BMP signalling but also other signalling. Yet, it is an interesting finding that low doses of DM mildly increased proliferation (Fig. 2A and B), suggesting that mild and specific inhibition of BMP signalling increased proliferative activity. The multiphasic effect of BMP signalling at low doses of DM was more clearly observed in IL-2 production in Jurkat cells, although this needs to be addressed by more sensitive means. Importantly, DM suppressed IL-2 production in mouse $CD4^+$ T cells in low doses with an IC_{50} similar to the one for the phosphorylation of Smad1/5/8, suggesting that IL-2 was a direct target of the BMP-SMAD signalling in these cells.

The analysis of RUNX1 and phospho-RUNX1 proteins suggests that RUNX1 is an important downstream target of BMP signalling in T cells. The level of the phosphorylated form, but not the total amount, of RUNX1 was decreased at the high dose of DM (5 μM, Fig. 7), where IL-2 production was profoundly suppressed (Fig. 6). We previously reported that RUNX1 was involved in IL-2 transcription, and that knockdown of RUNX1 completely suppressed IL-2 production in Jurkat cells [15]. Thus, it is interesting that the suppression of IL-2 by DM is coupled with the decrease of the phosphorylated form of RUNX1. Also, this result

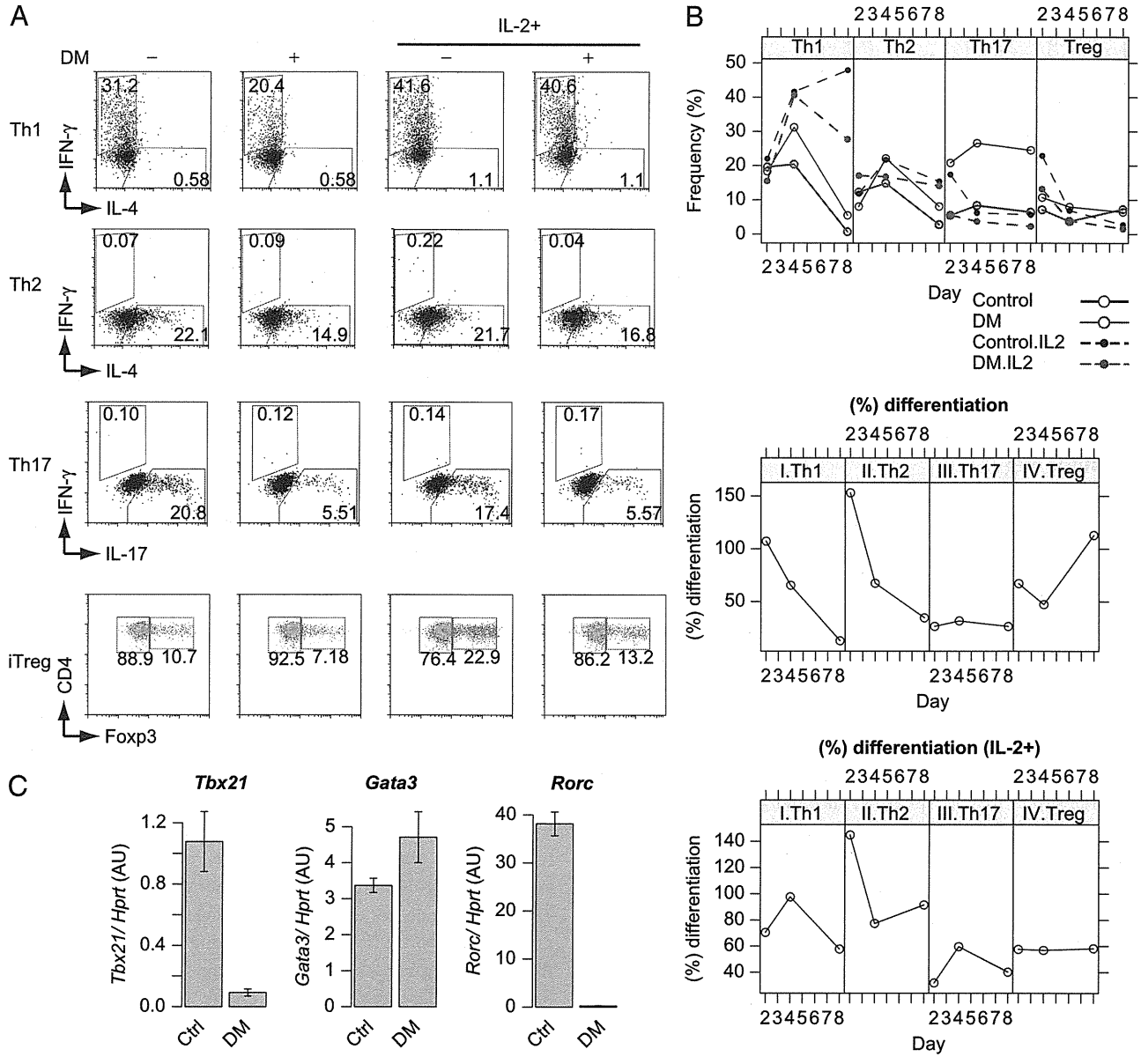

Figure 5. Perturbation effects of DM on Th/Treg differentiation. (A) $CD4^+CD25^-$ T cells were cultured with APCs and soluble anti-CD3 antibody, with DM (5 μM) or DMSO as a control, under indicated polarization conditions for 4 days. Cells were then restimulated with PMA and ionomycin for last 6 h, stained for intracellular cytokines, and analysed by flow cytometry. (B) Time course analysis of Th/Treg differentiation of DM-treated T cells. The frequency of polarized T cells (top), and % differentiation (middle and bottom) are shown. The latter is the value normalized to the percentage of control cells. For the gating strategy, see Supporting Information Fig. 1B. (C) Expression of the lineage-specific transcription factors. $CD4^+CD25^-$ naïve T cells were cultured with DM or DMSO as a control under the indicated conditions for 12 h, and levels of *Tbx21*, *GATA3*, *RORC* were measured by qPCR. *HPRT* was used as a reference gene. Data are shown as mean ± SD of triplicates. Representative results of three (A, B) or two (C) independent experiments are shown.

suggests that the phosphorylated form of RUNX1 is its activated form as suggested by a previous study [16]. Although we cannot exclude the possibility that DM directly suppressed nuclear kinases that phosphorylate RUNX1, this seems unlikely, given that rBMP2 upregulated the level of p-RUNX1 (Fig. 7D). The fact that treatment with rNoggin suppressed IL-2 production in the absence of rBMP2 indicates that in Jurkat cells endogenous BMP secretion signals for IL-2 production. Our study suggests that RUNX1 integrates the milieu of BMPs and its related proteins including Noggin via receiving BMP signalling.

Although further studies are required, BMP ligands and related morphogens from APCs may make morphogen milieus to modulate the differentiation and activation processes of T cells. Previous reports indicate that BMP-2, -4 and -7, and its endogenous inhibitors, Noggin and Chordin, are expressed in thymic epithelial cells

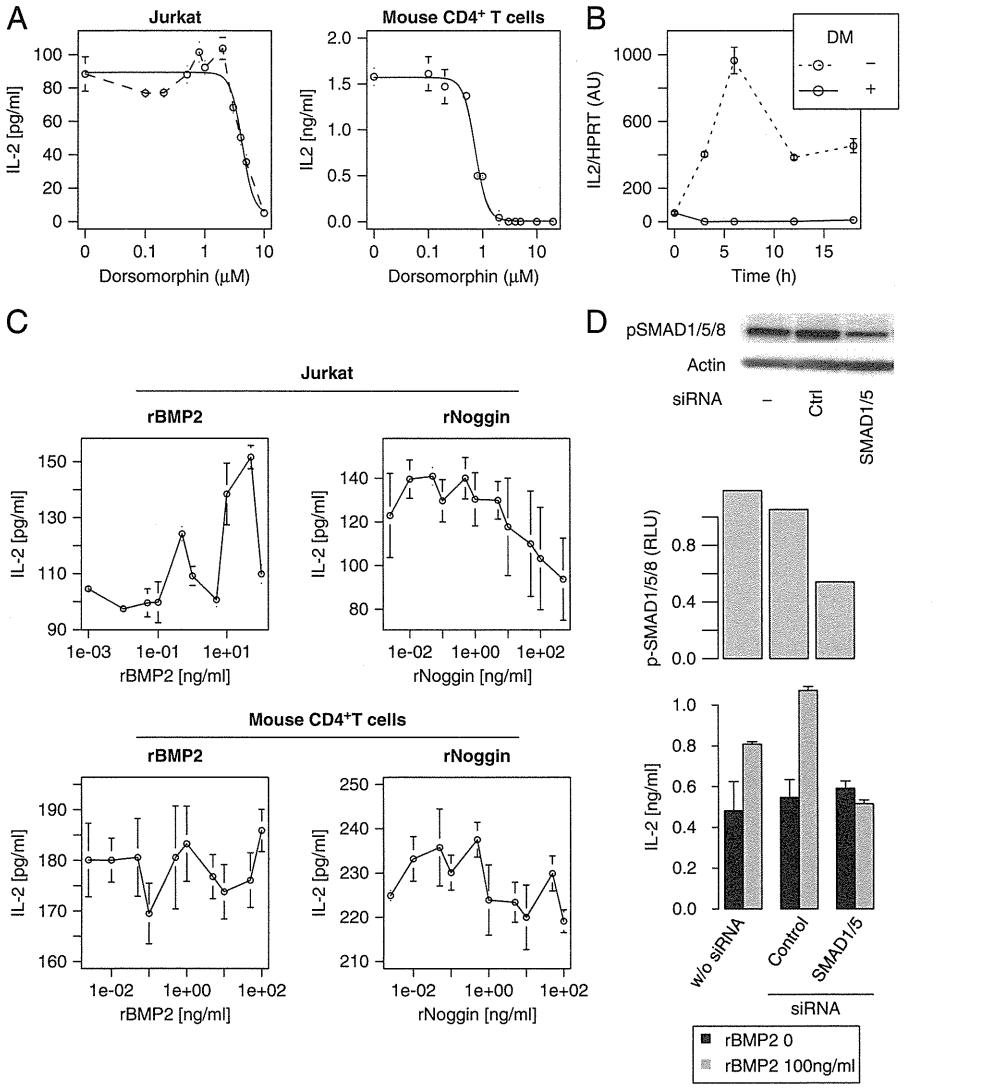

Figure 6. IL-2 production and transcription in DM-treated T cells. (A) Jurkat or mouse CD4$^+$ T cells were cultured for 18 h with DM or DMSO as a control, anti-CD3 and -CD28 antibodies. Data were regressed to a four-parameter log-logistic function (solid line). Points at low doses of DM in Jurkat cells were poorly fit to the log-logistic function, as demonstrated by dashed line. (B) Jurkat cells were stimulated for 3–18 h by anti-CD3 and -CD28 antibodies with DM (5 μM) or DMSO as a control. Relative levels of *Il2* were measured by qPCR. (C) Jurkat or mouse CD4$^+$ T cells were stimulated for 18 hours by anti-CD3 and -CD28 antibodies with titrated doses of recombinant BMP2 protein (rBMP2) or recombinant Noggin protein (rNoggin). IL-2 concentration in the culture supernatant was measured by ELISA. (D) IL-2 production by untreated cells (w/o siRNA) and siRNA-transduced Jurkat cells (control or SMAD1/5-siRNA) with or without rBMP2. Western blotting of pSMAD1/5/8 and actin using siRNA-transduced and non-transduced cells is shown (top). Densitometric analysis of the results of Western blotting of pSMAD1/5/8 and actin is shown (middle). IL-2 production of siRNA-transduced and non-transduced cells with or without rBMP2 (100 ng/mL) is shown (bottom). Data are shown as mean ± SD of triplicates. Representative results of three (A, B) or two (C, D) independent experiments are shown.

[2, 3]. We have found that some BMP ligands and their antagonists are expressed by various immunocytes. For example, monocytes express significantly higher amounts of Chordin (*Chrd*) mRNA than all other cell populations analysed in the data set of T cells, B cells, NK cells, Granulocytes, monocytes, and hematopoietic stem cells (GSE6506, [20]). Also, among B cells, plasma cells express much higher amounts of *Bmp1* and *Gdf2* compared with naïve B cells in the data set GSE4142 [21]. Further studies are required to find biological significance of the expression of these genes and understand the morphogen milieus in the immune system and their influence on T-cell differentiation in vivo.

In conclusion, we show that BMP signalling is involved in T-cell function and differentiation. DM, a specific inhibitor of BMPR (which does not inhibit TGF-β signalling) suppressed specific processes in T-cell activation and differentiation, and induced unique processes in treated cells. We described differential effects of DM and Noggin on T-cell activation and differentiation, demonstrating a physiological role for BMP signalling in these processes

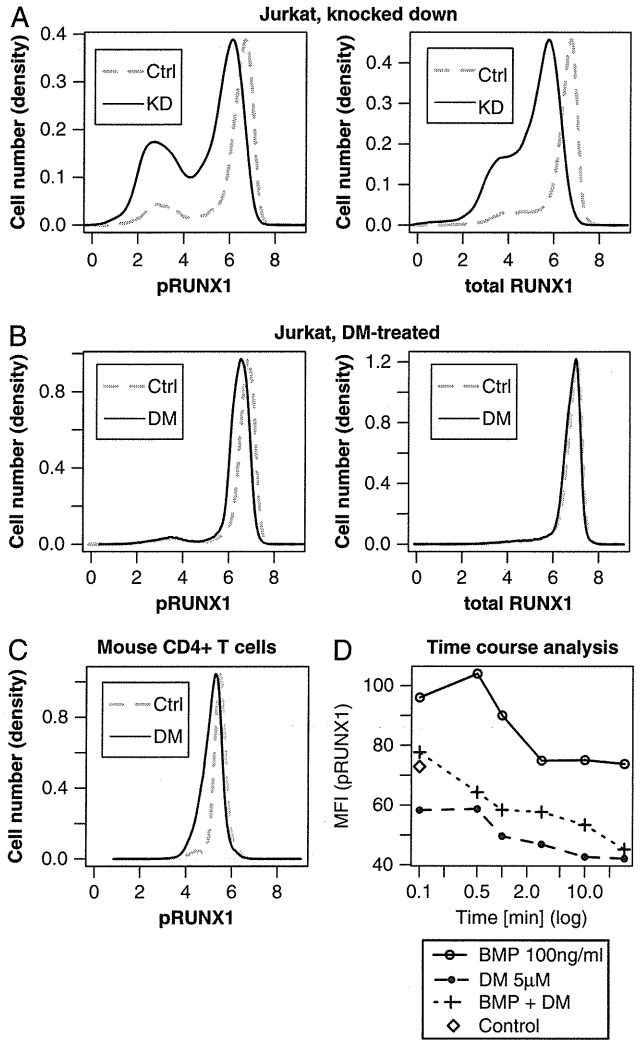

Figure 7. Regulation of phosphorylation of RUNX1/AML1 by BMP signalling. (A) Validation of anti-phospho-RUNX1 (pRUNX1) and -total RUNX1 antibodies. Jurkat cells were transduced with either RUNX1-siRNA (KD) or control siRNA (Ctrl) and cultured for 48 h. Knocked down cells were intracellularly stained by either anti-pRUNX1 or -total RUNX1 antibodies, and subsequently analysed by flow cytometry. (B) Jurkat cells were cultured for 3 h with DM (DM) or DMSO as a control (Ctrl), and subsequently stained by either anti-pRUNX1 or anti-total RUNX1 antibodies. (C) Mouse $CD4^+$ T cells were cultured for 3 h with DM or DMSO as a control, and stained by anti-pRUNX1 antibody. (D) Time course analysis of levels of pRUNX1 in Jurkat cells with rBMP2 and DM or DMSO. Jurkat cells were treated with rBMP2 (100 ng/mL) and either DM (5 μM) or DMSO, and analysed for pRUNX1. Representative results of two (A–C) or three (D) independent experiments are shown.

Materials and methods

Mouse, culture, and cell sorting

BALB/c mice were purchased from Japan SLC (Shizuoka, Japan), maintained under specific pathogen-free conditions in accordance with our institutional guidelines for animal welfare, and were used between 5 and 8 wks of age. $CD4^+$ T cells were isolated and cultured as previously described [15]. For CFSE dilution assay, magnetically sorted mouse $CD25^-CD4^+$ T cells were labeled with 3 μM CFSE (Dojindo and Invitrogen). Irradiated, magnetically sorted mouse $CD4^-CD90.2^-$ cells were used as APCs. DM was purchased from Calbiochem (San Diego).

Quantitative real-time PCR

Total RNA extracted and quantitated as previously described [15]. Primers used for human samples are the followings: *IL-2*, forward: 5′-TGCAACTCCTGT CTTGCATT-3′, reverse: 5′-TCCTG-GTGAGTTT GGGATTC-3′. *HPRT*, forward: 5′-GCTGAGGAT TTG-GAAAGGGTG-3′, reverse: 5′-TGAGCACAC AGAGGGCTACAATG-3′. Primers used for mouse sample are the followings: *Il2*, forward: 5′-CCTGAGCAGGATGGAGAATTACA-3′, reverse: 5′-TCCAGAACATGCCGCAGAG-3′. *Tbx21*, forward: 5′-CAACAAC-CCCTTTGCCAA AG-3′, reverse: 5′-TCCCCCAAGCAGTTGACAG T-3′. *Gata3*, forward: 5′-AGAACCGGCCCCTTA TGAA-3′, reverse: 5′-AGTTCGCGCAGGATGT CC-3′. *Rorc*, forward: 5′-ACCTCCA-CTGCCA GCTGTGTGCTGTC-3′, reverse: 5′-TCATTTCT GCACTT-CTGCATGTAGACTGTC-3′. *HPRT*, forward: 5′-TGAAGAGCTACT-GTAATGATC AGTCAAC-3′, reverse: 5′-AGCAAGCTTGCAAC CTT-AACCA-3′

Western blotting and ELISA

Western blotting and ELISA were preformed as previously described [15]. The following antibodies were used for immunoblot: anti-phospho SMAD1/5/8 (Cell Signallng Technology, Danvers, MA, USA), anti- SMAD1 (Millipore, Billerica, MA, USA), anti-phospho SMAD2 (Cell Signaling Technology), anti-SMAD2/3 (Cell Signaling Technology), anti- $p27^{Kip1}$ (BD Bioscience, San Jose, CA, USA), or anti- Actin (Millipore). IL-2 was measured by ELISA with BD OptEIA™, Human IL-2 ELISA (BD) or Mouse IL-2 ELISA (eBiosciene, San Diego, CA, USA)

Flow cytometric analysis of cell cycle and apoptosis

Cells were fixed with 70% ethanol, denatured, and stained with 7-Amino-actinomycin D (7AAD, Beckman Coulter, Brea, CA, USA), FITC Mouse IgG1k isotype control (MOPC-21, BD Pharmingen), FITC Mouse Anti-BrdU, (3D4, BD Pharmingen). For Annexin staining, cells were stained with Annexin V-FITC (Beckman Coulter), and 7AAD, according to manufacturer's instructions

Flow cytometric analysis of RUNX1

Anti-human and mouse phospho-AML1/RUNX1 (pS249, M93-568.4.27) and anti-human AML1/RUNX1 (N11- 683.51.51) are

generous gifts from BD Pharmingen. Cells were fixed and stained by using Fixation/Permeabilization concentrate (eBioscience), and were subsequently analysed by flow cytometry

Knockdown of AML1/RUNX1 and SMAD1/5

For AML1/RUNX1, Jurkat cells were transduced with AML1/RUNX1 siRNA (Stealth Select RNAi™ siRNA, Invitrogen) or control siRNA (Stealth RNAi™ siRNA Negative Control Hi GC) by the Amaxa nucleofector system according to the manufacturer's instruction. Transduced cells were cultured for 48 hours in the medium, and were subsequently stimulated for 3 h with plate-bound anti-CD3- and soluble anti-CD28-antibodies. Subsequently, cells were stained by either anti-AML1/RUNX1 or anti-phospho-AML1/RUNX1 (by anti-phospho- AML1/RUNX1 only in murine T cells), and were analysed by flow cytometry. For knockdown of SMAD1/5, Jurkat cells were transduced with a mixed siRNA for SMAD1 and SMAD5 (Stealth Select RNAi™) or control siRNA (Stealth RNAi™ siRNA Negative Control Lo GC)

Time course analysis of phopho-AML1/RUNX1

Cells were pre-heated in 2% FCS/PBS at 37°C for 3 min. Subsequently, recombinant BMP2 protein (100 ng/mL), and/or DM (5 μM), or DMSO, were added, and cells were incubated for indicated times. Immediately after incubation, cells were dipped in pre-warmed fixation buffer (BD Phosflow Fix Buffer I, BD bioscience), and incubated for 10 min in 37°C. Subsequently, cells were placed on ice for 30 min. Control cells were prepared with neither BMP2 nor DM, but with an equivalent amount of DMSO, and were fixed for 10 min in 37°C. Cells were permeabilised with chilled (−20°C) buffer (BD Phosflow Perm III Buffer, BD Bioscience) and stained with antibodies

Th/Treg polarization

Freshly sorted mouse $CD25^{-}CD4^{+}$ T cells (5×10^4) were co-cultured with APC (1×10^5) in the presence of 0.5 μg/mL soluble anti-CD3 monoclonal antibody (mAb). In addition, the following pairs of recombinant cytokines (20 ng/mL) and monoclonal mAbs (10 μg/mL) were added: rIL-12 and anti-IL-4 mAb For Th1; rIL-4, anti (IFNL-γ mAb for Th2; rIL-1β, rIL-6, rTGFβ, anti IL-4 mAb, and anti IFN-γ mAb for Th17; TGFL-β and rIL-2 (100 IU/mL, generous gift from Shionogi) for iTreg. Cytokines and Foxp3 were stained as previously described [15]

Microarray analysis

Mouse $CD4^{+}$ T cells were prepared and cultured with or without stimulation by plate bound anti-CD3 mAb and soluble anti-CD28 mAb for 1 h. Subsequently, 4 μM DM or DMSO was added and cells were incubated for 6 h. Total RNA was isolated as previously described [15]. Microarray data are available from the NCBI Gene Expression Omnibus (GEO) repository under the series accession number GSE27378

Bioinformatics for flow cytometric data

Flow cytometric data in Fig. 3A were processed by *flowCore* [22]. Data were normalised for the FL2 channel data (7AAD) by *flowStats* [23], using all the control and experimental groups stained with 7AAD and with or without BrdU-FITC. *FlowStats* normalises FCS data by adjusting the peaks of the channel data used for normalisation. By this normalisation process, the variance of the biphasic signals of 7AAD between samples was minimised without affecting FL1 data, thus enabling exactly same gating for G0/1, S, M, and subG0 in all the samples analysed. Normalised data were visualised by *flowViz* [24]. For CFSE data in Fig. 2, flowJo was used for model fit. The Mann–Whitney *U*-test was used for comparing unpaired flow cytometric data of two groups

Analysis of dose–response curve

Chemiluminescence intensities were quantified by *ImageJ*. Regression analysis for dose response curve was performed by the CRAN package *drc* [25]. Dose response data were fit to the four-parameter log-logistic function, *LL.4* in *drc*, by the following equation (x is the dose).

$$f(x,a,b,c,d) = c + \frac{d-c}{1+e^{b(\log(x)-\log(a))}}$$

.

Acknowledgements: We would like to give our thanks to Prof. Tessa Crompton for discussion, advice, and critical reading of the manuscript, Prof. Robin Callard, Dr. Tomoyuki Yamaguchi, and Dr. Takashi Nomura for comments on the manuscript. This work was supported by Grant-in-Aid for Specially Promoted Research, and grants-in-aid for Scientific Research on Priority Areas from the Ministry of Education, Culture, Sports, Science and Technology of Japan. MO is a Human Frontier Science Program Long-Term Fellow.

Conflict of interest: The authors declare no commercial or financial conflict of interest.

References

1 Chen, D., Zhao, M. and Mundy, G. R., Bone morphogenetic proteins. *Growth Factors* 2004. **22**: 233–241.

2 Hager-Theodorides, A. L., Outram, S. V., Shah, D. K., Sacedon, R., Shrimpton, R. E., Vicente, A., Varas, A. et al., Bone morphogenetic protein 2/4 signaling regulates early thymocyte differentiation. *J. Immunol.* 2002. **169**: 5496–5504.

3 Graf, D., Nethisinghe, S., Palmer, D. B., Fisher, A. G. and Merkenschlager, M., The developmentally regulated expression of Twisted gastrulation reveals a role for bone morphogenetic proteins in the control of T-cell development. *J. Exp. Med.* 2002. **196**: 163–171.

4 Lu, L., Ma, J., Wang, X., Wang, J., Zhang, F., Yu, J., He, G. et al., Synergistic effect of TGF-b superfamily members on the induction of Foxp3$^+$ Treg. *Eur. J. Immunol.* 2010. **40**: 142–152.

5 Kawabata, M., Imamura, T. and Miyazono, K., Signal transduction by bone morphogenetic proteins. *Cytokine Growth Factor Rev.* 1998. **9**: 49–61.

6 Miyazono, K., Maeda, S. and Imamura, T., BMP receptor signaling: transcriptional targets, regulation of signals, and signaling cross-talk. *Cytokine Growth Factor Rev.* 2005. **16**: 251–263.

7 Lee, K. S., Kim, H. J., Li, Q. L., Chi, X. Z., Ueta, C., Komori, T., Wozney, J. M. et al., Runx2 is a common target of transforming growth factor b1 and bone morphogenetic protein 2, and cooperation between Runx2 and Smad5 induces osteoblast-specific gene expression in the pluripotent mesenchymal precursor cell line C2C12. *Mol. Cell. Biol.* 2000. **20**: 8783–8792.

8 Pimanda, J. E., Donaldson, I. J., de Bruijn, M. F., Kinston, S., Knezevic, K., Huckle, L., Piltz, S. et al., The SCL transcriptional network and BMP signaling pathway interact to regulate RUNX1 activity. *Proc. Natl. Acad. Sci. USA* 2007. **104**: 840–845.

9 Lee, K. S., Hong, S. H. and Bae, S. C., Both the Smad and p38 MAPK pathways play a crucial role in Runx2 expression following induction by transforming growth factor-beta and bone morphogenetic protein. *Oncogene* 2002. **21**: 7156–7163.

10 Hong, C. C. and Yu, P. B., Applications of small molecule BMP inhibitors in physiology and disease. *Cytokine Growth Factor Rev.* 2009. **20**: 409–418.

11 Yu, P. B., Hong, C. C., Sachidanandan, C., Babitt, J. L., Deng, D. Y., Hoyng, S. A., Lin, H. Y. et al., Dorsomorphin inhibits BMP signals required for embryogenesis and iron metabolism. *Nat. Chem. Biol.* 2008. **4**: 33–41.

12 Rudd, C. E., Cell cycle 'check points' T-cell anergy. *Nat. Immunol.* 2006. **7**: 1130–1132.

13 Bindea, G., Mlecnik, B., Hackl, H., Charoentong, P., Tosolini, M., Kirilovsky, A., Fridman, W. H. et al., ClueGO: a Cytoscape plug-in to decipher functionally grouped gene ontology and pathway annotation networks. *Bioinformatics* 2009. **25**: 1091–1093.

14 Komine, O., Hayashi, K., Natsume, W., Watanabe, T., Seki, Y., Seki, N., Yagi, R. et al., The Runx1 transcription factor inhibits the differentiation of naïve CD4$^+$ T cells into the Th2 lineage by repressing GATA3 expression. *J. Exp. Med.* 2003. **198**: 51–61.

15 Ono, M., Yaguchi, H., Ohkura, N., Kitabayashi, I., Nagamura, Y., Nomura, T., Miyachi, Y. et al., Foxp3 controls regulatory T-cell function by interacting with AML1/Runx1. *Nature* 2007. **446**: 685–689.

16 Aikawa, Y., Nguyen, L. A., Isono, K., Takakura, N., Tagata, Y., Schmitz, M. L., Koseki, H. et al., Roles of HIPK1 and HIPK2 in AML1- and p300-dependent transcription, hematopoiesis and blood vessel formation. *EMBO J.* 2006. **25**: 3955–3965.

17 Sivertsen, E. A., Huse, K., Hystad, M. E., Kersten, C., Smeland, E. B. and Myklebust, J. H., Inhibitory effects and target genes of bone morphogenetic protein 6 in Jurkat TAg cells. *Eur. J. Immunol.* 2007. **37**: 2937–2948.

18 Varas, A., Sacedon, R., Hidalgo, L., Martinez, V. G., Valencia, J., Cejalvo, T., Zapata, A. et al., Interplay between BMP4 and IL-7 in human intrathymic precursor cells. *Cell Cycle* 2009. **8**: 4119–4126.

19 Hao, J., Ho, J. N., Lewis, J. A., Karim, K. A., Daniels, R. N., Gentry, P. R., Hopkins, C. R. et al., In vivo structure-activity relationship study of dorsomorphin analogues identifies selective VEGF and BMP inhibitors. *ACS Chem. Biol.* 2010. **5**: 245–253.

20 Chambers, S. M., Boles, N. C., Lin, K. Y., Tierney, M. P., Bowman, T. V., Bradfute, S. B., Chen, A. J. et al., Hematopoietic fingerprints: an expression database of stem cells and their progeny. *Cell Stem Cell* 2007. **1**: 578–591.

21 Luckey, C. J., Bhattacharya, D., Goldrath, A. W., Weissman, I. L., Benoist, C. and Mathis, D., Memory T and memory B cells share a transcriptional program of self-renewal with long-term hematopoietic stem cells. *Proc. Natl. Acad. Sci. USA* 2006. **103**: 3304–3309.

22 Ellis, B., Haaland, P., Hahne, F., Le Meur, N. and Gopalakrishnan, N., flowCore: Basic structures for flow cytometry data. *R package version* 1.14.1.

23 Hahne, F., Gopalakrishnan, N., Khodabakhshi, A. H. and Wong, C. J., flowStats: Statistical methods for the analysis of flow cytometry data. *R package version* 1.6.0.

24 Ellis, B., Gentleman, R., Hahne, F., Le Meur, N. and Sarkar, D., flowViz: Visualization for flow cytometry. *R package version* 1.12.0.

25 Ritz, C. and Streibig, J. C., Bioassay Analysis using R. *J. Stat. Software* 2005. **12**.

Abbreviations: **7AAD:** 7-amino-actinomycin D · **ActRII:** activin type II receptor · **AML1:** acute myeloid leukemia 1 · **BMP:** bone morphogenic protein · **BMPR:** BMP receptor · **DEGs:** differentially expressed genes · **DM:** dorsomorphin · **DN:** double negative · **DP:** double positive · **iTreg:** induced regulatory T cell · **MAPK:** mitogen-activated protein kinase · **qPCR:** quantitative real-time PCR · **rBMP2:** recombinant BMP2 · **rNoggin:** recombinant Noggin · **RUNX1:** runt-related transcription factor 1

Full correspondence: Dr. Masahiro Ono, Immunobiology Unit, Institute of Child Health, University College London, 30 Guilford Street, London WC1N 1EH, UK
Fax: +44-20-7905-2882
e-mail: m.ono@ucl.ac.uk

Received: 28/4/2011
Revised: 7/10/2011
Accepted: 21/11/2011
Accepted article online: 20/12/2011

Cancer Letters 310 (2011) 129–133

Contents lists available at ScienceDirect

Cancer Letters

journal homepage: www.elsevier.com/locate/canlet

Mini-review

Ovarian clear cell carcinoma as a stress-responsive cancer: Influence of the microenvironment on the carcinogenesis and cancer phenotype

Masaki Mandai *, Noriomi Matsumura, Tsukasa Baba, Ken Yamaguchi, Junzo Hamanishi, Ikuo Konishi

Department of Gynecology and Obstetrics, Kyoto University Graduate School of Medicine, 54 Shogoin Kawahara-cho, Sakyo-ku, Kyoto 606-8507, Japan

ARTICLE INFO

Article history:
Received 10 May 2011
Received in revised form 27 June 2011
Accepted 29 June 2011

Keywords:
Ovarian cancer
Endometriosis
Clear cell carcinoma
Microenvironment
Oxidative stress
Microarray
Pathogenesis

ABSTRACT

Although it is well known that ovarian endometriosis occasionally gives rise to ovarian cancers with specific histology such as endometrioid and clear cell carcinomas, its etiology is not fully understood. We have shown that a stressful microenvironment within the endometriotic cyst may lead to cancer development by inducing unique gene expressions, which potentially serves as a molecular marker for treatment modality. In this review, by referring to other articles in this field, we explore how the carcinogenic microenvironment affects the phenotype and gene expression of a cancer, and how we can develop new treatment based on this concept.

1. Introduction

Endometriosis is a benign gynecological disease that affects 5–10% of women [1]. It is clinically well known that ovarian cancer arises from ovarian endometriosis with a relatively high frequency. A prospective randomized trial in Japan, in which over 8000 asymptomatic postmenopausal women were followed for up to 17 years, demonstrated that 0.72% of women with endometriosis develop ovarian cancer [2]. This rate is higher than the incidence of cancer in other benign ovarian tumors such as serous or mucinous cystoadenomas [2], suggesting the presence of discrete risk factors for oncogenesis in ovarian endometriosis. In addition, unlike typical ovarian cancers, the cancers arising from endometriosis more commonly comprise clear cell and endometrioid subtypes [3,4]. These findings strongly suggest that the carcinogenic process in ovarian endometriosis is unique and different from that of ordinary ovarian cancers. With this in mind, we sought to clarify the mechanism by which endometriosis gives rise to a discrete phenotype of cancer with a high frequency, and we hypothesized that the unique microenvironment in the endometriotic cyst plays a pivotal role in cancer development.

Pathological evidences as well as recent molecular analyses have been clarifying the precancerous property of endometriosis. Pathologically, co-existence of endometriosis and ovarian cancer is frequently observed, and they sometimes accompany "atypical endometriosis", a putative precursor lesion [5]. Common genetic events such as LOH and genetic mutation have been demonstrated in carcinoma and adjacent endometriosis [5]. Overexpression of HNF-1β, a putative hallmark of clear cell carcinoma, is also frequently expressed in benign and atypical endometriosis [6]. Moreover, mutation of the ARID1A gene, which is recently identified in approximately a half of clear cell carcinoma and one thirds of endometrioid carcinoma, is also found in a part of atypical endometriosis adjacent to the carcinoma [7]. These data collectively suggest that endometriosis really transform into carcinoma, occasionally

* Corresponding author. Tel.: +81 75 751 3269; fax: +81 75 761 3967.
E-mail address: mandai@kuhp.kyoto-u.ac.jp (M. Mandai).

0304-3835/$ - see front matter © 2011 Elsevier Ireland Ltd. All rights reserved.
doi:10.1016/j.canlet.2011.06.039

passing through an intermediate lesion, namely, atypical endometriosis. However, little is known about the mechanisms that drive benign epithelium into malignant transformation within the endometriotic cyst.

2. High iron concentration and its potential influence in the development of ovarian cancer in endometriosis

Endometriosis is characterized by repeated bleeding into the cyst cavity during the menstrual cycle. As a result, the content of an endometriotic cyst consists of highly concentrated old blood, and the endometriotic epithelial cells within the cyst are consistently exposed to an unusual microenvironment that is rarely encountered in the body. Recently it has been recognized that carcinogenesis and tumor progression are significantly influenced by the microenvironment in which the tumor arises [8,9]. We therefore sought to identify elements specifically included in the cystic fluid of endometriosis. As expected, the concentration of iron was markedly high in endometriotic cysts [10], in accordance with previous reports [11,12]. In our study, the free iron concentration was also markedly high in endometriotic cysts compared with other benign ovarian cysts. Free iron is associated with cancer development through induction of persistent oxidative stress in several organs such as liver and lung [13,14]. There is also a ferric nitrilotriacetate-induced renal carcinogenesis model that shows the contribution of catalytic iron to cancer development [15]. Therefore, persistent exposure to highly concentrated free iron may lead to ovarian cancer, possibly via production of oxidative stress.

To examine this possibility further, we evaluated the extent of oxidative stress within the endometriotic cyst compared to other benign ovarian tumors. Lactose dehydrogenase (LDH), a marker of tissue damage; potential antioxidant (PAI), an antioxidant marker; lipid peroxidase (LPO), a marker of oxidative stress; and 8-hydroxy-2-deoxyguanosine, a marker of DNA damage; were all significantly elevated in endometriotic cysts compared with other ovarian cysts [10]. Obviously, the epithelial cells within the endometriotic cyst are exposed to extensive oxidative stress (reactive oxygen species, ROS), and as a result, they are subjected to more cellular and DNA damage than other benign ovarian tumors (Fig. 1). Actually, our *in vitro* experiments revealed that the fluid in chocolate cysts is more mutagenic than that of other cysts [10]. Hence, epithelial cells within the endometriotic cyst are subject to "microenvironment-induced mutagenesis" [15]. The link between the stressful microenvironment and cancer development is supported by several other reports. (1) Chromosomal aberrations are present at a higher frequency in ovarian endometriotic cysts compared to extra-gonadal endometriosis where the epithelium is less exposed to old blood elements [16]. (2) The occurrence of ovarian cancer increases with the duration of endometriosis [17].

It is, of course, an oversimplification to ascribe the cause of cancer development in endometriosis solely to the accumulated iron. The characteristic microenvironment within the endometriotic cyst may include other factors such as hypoxia, poor nutrition or altered immune status (Fig. 1). Hypoxia, for instance, also increases ROS leading to increased DNA damage and less efficient DNA repair [18,19]. To investigate these aspects further, more comprehensive analyses using genome-wide analysis was needed.

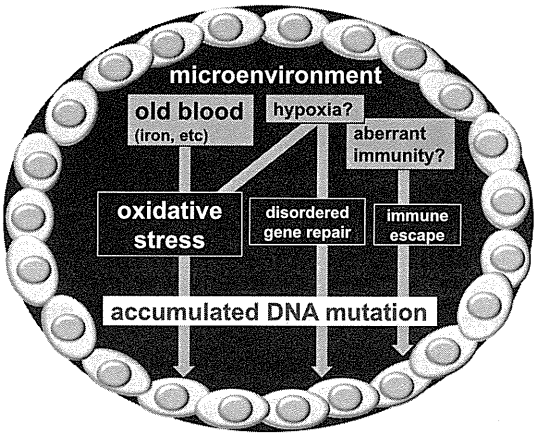

Fig. 1. Influence of the microenvironment within the endometriotic cyst on carcinogenesis. Fluid in the endometriotic cyst contains various special elements including free iron and constitutes a unique stressful microenvironment, which thereby leads to the cancer development.

3. Influence of microenvironment on the gene expression and phenotype of cancer arising in endometriosis

There is likely to be an association between endometrioid adenocarcinoma and endometriosis because of the similarity to the relationship between endometrioid adenocarcinoma and the uterine endometrium. Several studies suggest the etiological role of estrogen in both cases [20]. In contrast, no clear explanation has been found for the observation that clear cell carcinoma frequently occurs in endometriosis.

We then hypothesized that the microenvironment within the endometriosis, which appears to be associated with the development of ovarian cancer, also affects the phenotype of the cancer arising there. To verify this possibility, we first identified the gene signature that distinguishes clear cell carcinoma from other types of ovarian cancer using a microarray dataset of ovarian cancers [21]. The signature consisted of 437 genes and was designated as the ovarian clear cell carcinoma (OCCC) signature. It could efficiently distinguish clear cell carcinomas in multiple independent databases, indicating that the OCCC signature is indeed specific for clear cell carcinoma. Next, we analyzed what kinds of genes were included in this signature. A categorical analysis, Allez, demonstrated that genes belonging to three categories, stress response, sugar metabolism and coagulation, are frequently involved in this signature. Especially stress-related genes occupy a significant part, suggesting that they play a central role in the manifestation of the phenotypical features of clear cell carcinoma. Then, a computer-based pathway analysis was employed to elucidate the functional relationships among

the genes included in OCCC. Interestingly, one signal network consisting of a relatively large number of genes, including many stress-related genes such as HIF1-α, IL-6, and SOD2, was supposed to be activated in clear cell carcinoma. This result suggests that at least one of the major functions evoked by OCCC signature genes is the stress-response.

Our next question was whether the microenvironment within the endometriotic cyst is in any way associated with the expression of the OCCC signature. To address this question, we treated ovarian surface epithelial cells with the contents of endometriotic cysts and assessed the time-course of the alteration of the OCCC signature by microarray. The OCCC signature was induced by endometriotic fluid in a time dependent manner, which suggests that the OCCC signature is primarily a response of epithelial cells to the microenvironment within the endometriotic cyst [21]. If this is the case, the expression of the OCCC signature in the case of clear cell carcinoma should be based on some other mechanism than merely gene induction because they are constitutively expressed in clear cell carcinoma without any specific stress in the culture medium. We speculated that epigenetic regulation may have something to do with the constitutive expression of the OCCC signature and examined the methylation status in ovarian cancer cells. In two genes we examined, VCAN and HNF-1β, methylation in the regulatory region of the gene is more frequent in clear cell carcinoma than in serous carcinomas, suggesting that, at least in part, OCCC signature expression is caused by epigenetic alteration [21]. Thus, it is estimated that the OCCC signature should first be induced by the stressful environment in the endometriotic cyst and then fixed in the course of development of the clear cell carcinoma (Fig. 2).

Taken together, the identification and analysis of the OCCC signature gave us the idea that the specific microenvironment induces unique gene expressions and leads to a cancer of a special phenotype (Fig. 3). Recently, the effect of the local microenvironment such as ROS or inflammation was implicated in cancer development [22]. However, a link between the microenvironment and the occurrence

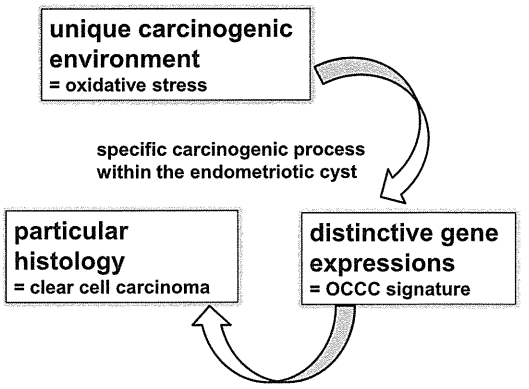

Fig. 3. A specific carcinogenic process within the endometriotic cyst. A stressful microenvironment not only induces carcinogenesis but also affects the phenotype and character of the cancer derived under its influence.

of a specific cancer phenotype is a new insight, and further evidence should be collected to verify this concept.

4. Possible application of the OCCC signature in the treatment of disease

Is it possible to apply the OCCC signature to the treatment of ovarian clear cell carcinoma? To answer this question, we evaluated the malignant tumors in the whole body to ascertain whether there are cancers with elevated expression of the OCCC signature [23]. Among various cancers, only renal cell carcinomas (RCC) express significantly higher levels of the OCCC signature. In hierarchical clustering using the OCCC signature, ovarian clear cell carcinoma was indistinguishable from RCC, indicating the similarity in gene expressions between these cancers. RCC is generally chemoresistant, and until recently, IFN-α and IL-2 were the only therapeutic agents clinically used for RCC, and they had only modest response rates [24]. However, the recently introduced molecular target drugs sorafenib and sunitinib provide significant therapeutic efficacy, drastically changing the modality of this tumor [25,26]. Given

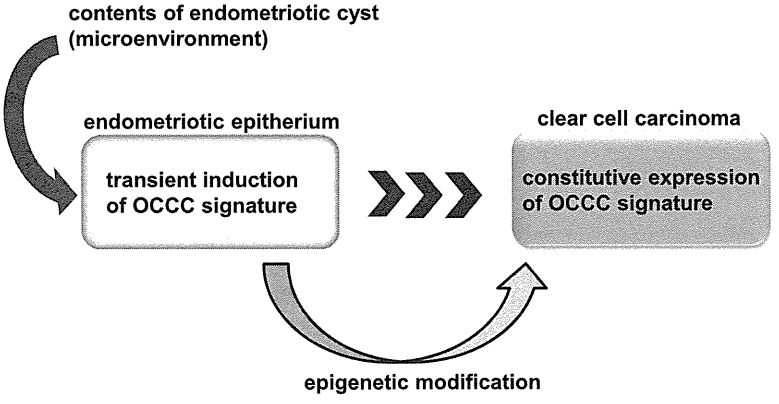

Fig. 2. Transient induction of the OCCC signature and subsequent fixation of the expression by epigenetic alteration. The expression of the OCCC signature is transiently induced in the presence of endometriotic fluid and subsequently becomes constitutive partly by epigenetic modifications.

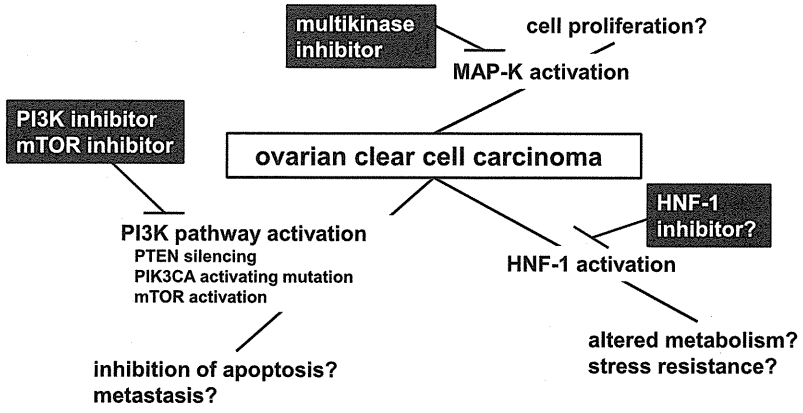

Fig. 4. Multimodality molecular targeting therapy for ovarian clear cell carcinoma. Clear cell carcinoma, a chemoresistant cancer, should be treated by multimodal targeting therapy based on the biological nature of the tumor.

the results indicating the similarity between OCCC and RCC, we sought to further investigate the efficacy of sorafenib and sunitinib against OCCC. A mouse xenograft model using the human OCCC cell line, RMG-2, which is known to be chemoresistant, clearly indicated that sorafenib is effective in the suppression of RMG-2.

We then evaluated the mechanism by which sorafenib exerts its antitumor effect. Sorafenib is known to inhibit multiple kinase activities, including those activated by epidermal growth factor receptor (EGFR), platelet derived growth factor receptor (PDGFR) and vascular endothelial growth factor receptor (VEGFR) [27,28]. In our analyses of various oncogenic pathways among ovarian cancers, OCCC is characterized by the activation of MAPK, while oncogenic signals related to cell proliferation, such as E2F3 and Myc, are not activated compared with other ovarian cancers such as serous adenocarcinoma. *In vitro* experiments revealed that sorafenib can inhibit the MAPK activity of RMG-2, in accordance with other reports [29,30], suggesting that this might be the primary consequence of the antitumor effect of sorafenib in our study. These data suggest that comprehensive assessment of specific gene expressions in one type of cancer provides a reasonable background for the selection of a therapeutic reagent that targets an activated intracellular signal, especially in the case of a slowly proliferating, chemoresistant tumor such as OCCC.

5. Further directions, especially future treatment approaches for clear cell carcinoma (Fig. 4)

Most of the clear cell carcinomas are resistant to current chemotherapy, and the treatment of this tumor remains an important clinical challenge in the treatment of ovarian cancer. As mentioned above, our comprehensive gene expression analyses revealed that the molecular targeting drugs effective for RCC are potentially useful in the treatment of OCCC, one of which is sorafenib. There are several other reagents that are expected to be effective in RCC, and such drugs are thought to be candidates for therapeutic reagents against OCCC. For instance, mTOR inhibitors (temsirolimus, everolimus) as well as VEGF signaling blockers (bevacizumab) are shown to be promising therapeutic reagents in RCC [31–33] (Fig. 4). Both are induced by HIF-1α activation, a fundamental feature in RCC harboring VHL aberrations [34].

Another possible target molecule in OCCC is HNF-1β. This molecule is known to be a specific marker for clear cell carcinoma [35]. In our analyses, HNF-1β is included in the OCCC signature and in the signal network estimated by pathway analysis [21]. Moreover, gene expression of this molecule is regulated by DNA methylation in cancer cells [21]. The DNA binding motifs of HNF-1β were significantly enriched in OCCC [23]. These data collectively suggest that HNF-1β plays a pivotal role in the biological behavior of OCCC. However, the precise function of this protein is not fully understood. To determine whether this molecule could be a therapeutic target, we are now evaluating the effect of suppressing the expression of this gene in HNF-1β-overexpressing OCCC cells.

Obviously, in a chemoresistant malignancy like OCCC, the future treatment modality consists mainly of combinations of the various molecular targeting drugs mentioned above. In this respect, the most important strategy in successfully applying those reagents in each case of OCCC is to reliably identify the molecular marker that can predict the efficacy of those reagents. The OCCC signature, which reflects the fundamental character of OCCC and represents the 'OCCC-likeness', might serve as such a marker. However, to estimate more precisely which drug is most effective in each case, it will be necessary to develop individual signatures to reflect signal pathways corresponding to each drug.

Conflict of interest

All the authors in this study do not have any financial and personal relationships with other people or organizations that could inappropriately influence (bias) our work.

References

[1] S.E. Bulun, Endometriosis, New Engl. J. Med. 360 (3) (2009) 268–279.
[2] H. Kobayashi, K. Sumimoto, N. Moniwa, M. Imai, K. Takakura, T. Kuromaki, E. Morioka, K. Arisawa, T. Terao, Risk of developing

ovarian cancer among women with ovarian endometrioma: a cohort study in Shizuoka, Japan, Int. J. Gynecol. Cancer 17 (1) (2007) 37–43.
[3] D.S. McMeekin, R.A. Burger, A. Manetta, P. DiSaia, M.L. Berman, Endometrioid adenocarcinoma of the ovary and its relationship to endometriosis, Gynecol. Oncol. 59 (1) (1995) 81–86.
[4] S. Komiyama, D. Aoki, E. Tominaga, N. Susumu, Y. Udagawa, S. Nozawa, Prognosis of Japanese patients with ovarian clear cell carcinoma associated with pelvic endometriosis: clinicopathologic evaluation, Gynecol. Oncol. 72 (3) (1999) 342–346.
[5] M. Mandai, K. Yamaguchi, N. Matsumura, T. Baba, I. Konishi, Ovarian cancer in endometriosis: molecular biology, pathology, and clinical management, Int. J. Clin. Oncol. 14 (5) (2009) 383–391.
[6] N. Kato, S. Sasou, T. Motoyama, Expression of hepatocyte nuclear factor-1beta (HNF-1beta) in clear cell tumors and endometriosis of the ovary, Mod. Pathol. 19 (1) (2006) 83–89.
[7] K.C. Wiegand, S.P. Shah, O.M. Al-Agha, Y. Zhao, K. Tse, T. Zeng, J. Senz, M.K. McConechy, M.S. Anglesio, S.E. Kalloger, W. Yang, A. Heravi-Moussavi, R. Giuliany, C. Chow, J. Fee, A. Zayed, L. Prentice, N. Melnyk, G. Turashvili, A.D. Delaney, J. Madore, S. Yip, A.W. McPherson, G. Ha, L. Bell, S. Fereday, A. Tam, L. Galletta, P.N. Tonin, D. Provencher, D. Miller, S.J. Jones, R.A. Moore, G.B. Morin, A. Oloumi, N. Boyd, S.A. Aparicio, I.e.M. Shih, A.M. Mes-Masson, D.D. Bowtell, M. Hirst, B. Gilks, M.A. Marra, D.G. Huntsman, ARID1A mutations in endometriosis-associated ovarian carcinomas, New Engl. J. Med. 363 (16) (2010) 1532–1543.
[8] T.L. Whiteside, The tumor microenvironment and its role in promoting tumor growth, Oncogene 27 (45) (2008) 5904–5912.
[9] E. Laconi, The evolving concept of tumor microenvironments, Bioessays 29 (8) (2007) 738–744.
[10] K. Yamaguchi, M. Mandai, S. Toyokuni, J. Hamanishi, T. Higuchi, K. Takakura, S. Fujii, Contents of endometriotic cysts, especially the high concentration of free iron, are a possible cause of carcinogenesis in the cysts through the iron-induced persistent oxidative stress, Clin. Cancer Res. 14 (1) (2008) 32–40.
[11] M. Iizuka, M. Igarashi, Y. Abe, Y. Ibuki, Y. Koyasu, K. Ikuma, Chemical assay of iron in ovarian cysts: a new diagnostic method to evaluate endometriotic cysts, Gynecol. Obstet. Invest. 46 (1) (1998) 58–60.
[12] K. Takahashi, S. Okada, M. Okada, M. Kitao, Y. Kaji, K. Sugimura, Magnetic resonance relaxation time in evaluating the cyst fluid characteristics of endometrioma, Hum. Reprod. 11 (4) (1996) 857–860.
[13] S. Adachi, S. Yoshida, K. Kawamura, M. Takahashi, H. Uchida, Y. Odagiri, K. Takemoto, Inductions of oxidative DNA damage and mesothelioma by crocidolite, with special reference to the presence of iron inside and outside of asbestos fiber, Carcinogenesis 15 (4) (1994) 753–758.
[14] S. Toyokuni, Role of iron in carcinogenesis: cancer as a ferrotoxic disease, Cancer Sci. 100 (1) (2009) 9–16.
[15] S. Toyokuni, T. Tanaka, Y. Nishiyama, K. Okamoto, Y. Nakashima, S. Hamazaki, S. Okada, H. Hiai, Induction of renal cell carcinoma in male Wistar rats treated with cupric nitrilotriacetate, Lab. Invest. 75 (2) (1996) 239–248.
[16] M. Körner, E. Burckhardt, L. Mazzucchelli, Higher frequency of chromosomal aberrations in ovarian endometriosis compared to extragonadal endometriosis: a possible link to endometrioid adenocarcinoma, Mod. Pathol. 19 (12) (2006) 1615–1623.
[17] A. Melin, P. Sparén, I. Persson, A. Bergqvist, Endometriosis and the risk of cancer with special emphasis on ovarian cancer, Hum. Reprod. 21 (5) (2006) 1237–1242.
[18] A. Coquelle, F. Toledo, S. Stern, A. Bieth, M. Debatisse, A new role for hypoxia in tumor progression: induction of fragile site triggering genomic rearrangements and formation of complex DMs and HSRs, Mol. Cell 2 (2) (1998) 259–265.
[19] A.X. Meng, F. Jalali, A. Cuddihy, N. Chan, R.S. Bindra, P.M. Glazer, R.G. Bristow, Hypoxia down-regulates DNA double strand break repair gene expression in prostate cancer cells, Radiother. Oncol. 76 (2) (2005) 168–176.
[20] M.A. Gates, B.A. Rosner, J.L. Hecht, S.S. Tworoger, Risk factors for epithelial ovarian cancer by histologic subtype, Am. J. Epidemiol. 171 (1) (2010) 45–53.
[21] K. Yamaguchi, M. Mandai, T. Oura, N. Matsumura, J. Hamanishi, T. Baba, S. Matsui, S.K. Murphy, I. Konishi, Identification of an ovarian clear cell carcinoma gene signature that reflects inherent disease biology and the carcinogenic processes, Oncogene 29 (12) (2010) 1741–1752.
[22] T.A. Gonda, S. Tu, T.C. Wang, Chronic inflammation, the tumor microenvironment and carcinogenesis, Cell Cycle 8 (13) (2009) 2005–2013.
[23] N. Matsumura, M. Mandai, T. Okamoto, K. Yamaguchi, S. Yamamura, T. Oura, T. Baba, J. Hamanishi, H.S. Kang, S. Matsui, S. Mori, S.K. Murphy, I. Konishi, Sorafenib efficacy in ovarian clear cell carcinoma revealed by transcriptome profiling, Cancer Sci. 101 (12) (2010) 2658–2663.
[24] D.F. McDermott, M.B. Atkins, Application of IL-2 and other cytokines in renal cancer, Expert Opin. Biol. Ther. 4 (4) (2004) 455–468.
[25] B. Escudier, T. Eisen, W.M. Stadler, C. Szczylik, S. Oudard, M. Staehler, S. Negrier, C. Chevreau, A.A. Desai, F. Rolland, T. Demkow, T.E. Hutson, M. Gore, S. Anderson, G. Hofilena, M. Shan, C. Pena, C. Lathia, R.M. Bukowski, Sorafenib for treatment of renal cell carcinoma: final efficacy and safety results of the phase III treatment approaches in renal cancer global evaluation trial, J. Clin. Oncol. 27 (20) (2009) 3312–3318.
[26] R.J. Motzer, T.E. Hutson, P. Tomczak, M.D. Michaelson, R.M. Bukowski, S. Oudard, S. Negrier, C. Szczylik, R. Pili, G.A. Bjarnason, X. Garcia-del-Muro, J.A. Sosman, E. Solska, G. Wilding, J.A. Thompson, S.T. Kim, I. Chen, X. Huang, R.A. Figlin, Overall survival and updated results for sunitinib compared with interferon alfa in patients with metastatic renal cell carcinoma, J. Clin. Oncol. 27 (22) (2009) 3584–3590.
[27] P.H. Patel, R.S. Chadalavada, R.S. Chaganti, R.J. Motzer, Targeting von Hippel–Lindau pathway in renal cell carcinoma, Clin. Cancer Res. 12 (24) (2006) 7215–7220.
[28] S. Wilhelm, C. Carter, M. Lynch, T. Lowinger, J. Dumas, R.A. Smith, B. Schwartz, R. Simantov, S. Kelley, Discovery and development of sorafenib: a multikinase inhibitor for treating cancer, Nat. Rev. Drug Discov. 5 (10) (2006) 835–844.
[29] L. Liu, Y. Cao, C. Chen, X. Zhang, A. McNabola, D. Wilkie, S. Wilhelm, M. Lynch, C. Carter, Sorafenib blocks the RAF/MEK/ERK pathway, inhibits tumor angiogenesis, and induces tumor cell apoptosis in hepatocellular carcinoma model PLC/PRF/5, Cancer Res. 66 (24) (2006) 11851–11858.
[30] R.N. Keswani, A. Chumsangsri, R. Mustafi, J. Delgado, E.E. Cohen, M. Bissonnette, Sorafenib inhibits MAPK-mediated proliferation in a Barrett's esophageal adenocarcinoma cell line, Dis. Esophagus 21 (6) (2008) 514–521.
[31] G. Hudes, M. Carducci, P. Tomczak, J. Dutcher, R. Figlin, A. Kapoor, E. Staroslawska, J. Sosman, D. McDermott, I. Bodrogi, Z. Kovacevic, V. Lesovoy, I.G. Schmidt-Wolf, O. Barbarash, E. Gokmen, T. O'Toole, S. Lustgarten, L. Moore, R.J. Motzer, Global ARCC Trial, Temsirolimus, interferon alfa, or both for advanced renal-cell carcinoma, New Engl. J. Med. 356 (22) (2007) 2271–2281.
[32] R.J. Motzer, B. Escudier, S. Oudard, T.E. Hutson, C. Porta, S. Bracarda, V. Grünwald, J.A. Thompson, R.A. Figlin, N. Hollaender, G. Urbanowitz, W.J. Berg, A. Kay, D. Lebwohl, A. Ravaud, RECORD-1 Study Group, Efficacy of everolimus in advanced renal cell carcinoma: a double-blind, randomised, placebo-controlled phase III trial, Lancet 372 (9637) (2008) 449–456.
[33] J.C. Yang, L. Haworth, R.M. Sherry, P. Hwu, D.J. Schwartzentruber, S.L. Topalian, S.M. Steinberg, H.X. Chen, S.A. Rosenberg, A randomized trial of bevacizumab, an anti-vascular endothelial growth factor antibody, for metastatic renal cancer, New Engl. J. Med. 349 (5) (2003) 427–434.
[34] P.E. Clark, The role of VHL in clear-cell renal cell carcinoma and its relation to targeted therapy, Kidney Int. 76 (9) (2009) 939–945.
[35] A. Tsuchiya, M. Sakamoto, J. Yasuda, M. Chuma, T. Ohta, M. Ohki, T. Yasugi, Y. Taketani, S. Hirohashi, Expression profiling in ovarian clear cell carcinoma: identification of hepatocyte nuclear factor-1 beta as a molecular marker and a possible molecular target for therapy of ovarian clear cell carcinoma, Am. J. Pathol. 163 (6) (2003) 2503–2512.

Clinical Immunology (2011) 141, 338–347

available at www.sciencedirect.com

Clinical Immunology

www.elsevier.com/locate/yclim

The comprehensive assessment of local immune status of ovarian cancer by the clustering of multiple immune factors

Junzo Hamanishi, Masaki Mandai*, Kaoru Abiko, Noriomi Matsumura, Tsukasa Baba, Yumiko Yoshioka, Kenzo Kosaka, Ikuo Konishi

Department of Gynecology and Obstetrics, Graduate School of Medicine, Kyoto University, 54 Shogoin Kawahara-cho, Sakyo-ku, Kyoto 606-8507, Japan

Received 12 April 2011; accepted with revision 26 August 2011
Available online 2 September 2011

KEYWORDS
Ovarian cancer;
Tumor immunity;
Tumor immune escape

Abstract The aim of this study was to evaluate the local immune status of human ovarian cancers by the comprehensive analysis of tumor-infiltrating immune cells and immunosuppressive factors, and to elucidate the local immunity in clinical course. The numbers of CD1α+, CD4+, CD8+, CD57+, forkhead box P3+ and programmed cell death-1+ cells were counted, and the intensity of immunosuppressive factors, such as programmed cell death-1 ligand (PD-L)1, PD-L2, cyclooxygenase (COX)-1, COX-2 and transforming growth factor β1, were evaluated in 70 ovarian cancer specimens stained by immunohistochemistry. Then hierarchical clustering of these parameters showed the four clusters into ovarian cancer cases. Cluster 1, which had significantly better prognosis than the others, was characterized by high infiltration of CD4+ and CD8+ cells. In conclusion the comprehensive analysis of local immune status led to subdivide ovarian cancers into groups with better or worse prognoses and may guide precise understanding of the local immunity.

1. Introduction

Ovarian cancer is the most lethal gynecologic cancer in the world with >200,000 patients diagnosed every year and over a half of them dying annually. These deaths are partly due to the fact that more than half of the patients with ovarian cancer are diagnosed at advanced tumor stages (stage III or IV). Although platinum or taxane-based chemotherapies are effective in the treatment of the majority of ovarian cancer cases, most of the patients suffer from recurrence and eventually develop chemo-resistance. Considering the high mortality rate of ovarian cancer due to the absence of curative treatment in the advanced stage or at recurrence,

* Corresponding author. Fax: +81 761 3967.
E-mail address: mandai@kuhp.kyoto-u.ac.jp (M. Mandai).

1521-6616/$ - see front matter © 2011 Elsevier Inc. All rights reserved.
doi:10.1016/j.clim.2011.08.013

new therapeutic modalities other than chemotherapy and surgery are urgently needed [1–3].

Tumor immune therapy has long been considered as an alternative modality in the treatment of solid tumors including ovarian cancer. Nevertheless, there have been few reports on clinically successful immune therapies. The failure in immune therapies in such clinical trials is partly ascribed to the phenomenon designated as "tumor immune escape". It is increasingly understood that the dynamic interaction between tumor cells and immune cells in the local microenvironment plays a pivotal role in cancer development and progression [4]. In the case of advanced cancers, tumor cells establish an immunosuppressive environment regionally and make it difficult to induce immune activation to eliminate cancer cells. In this situation, adoptive immunotherapy, such as a tumor vaccine, is not sufficient to eradicate tumors [5,6].

The differences in the phenotypes or populations of tumor-infiltrating immune cells, such as CD4+ (helper) T cells, CD8+ (cytotoxic) T cells, CD57+ (NK) cells and CD11c+ (dendritic) cells, have been shown to be associated with different clinical outcomes of solid tumors including colorectal cancer [7], breast cancer [8], gastric cancer [9,10], lung cancer [11,12], hepatic cancer [13,14], melanoma [15], kidney cancer [16] and uterine cervical cancer [17]. In ovarian cancer, several recent studies have shown an association between tumor-infiltrating immune cells and clinical outcomes [18,19]. We also reported that CD8+ T cell infiltration [20] and NK cell infiltration [21] are associated with a favorable prognosis in the ovarian cancer patient. On the other hand, regulatory T cells, most specific marker of which is FOXP3, in the tumor site play a suppressive role in the local tumor immunity, leading to tumor progression [22,23].

With respect to the tumor, there are also a wide variety of mechanisms that enable tumor cells to evade an immune attack. These mechanisms include a loss of MHC [24], the upregulation of immunosuppressive factors, such as transforming growth factor β (TGFβ) [25], IL-10, indoleamine 2,3-dioxygenase (IDO) [26] and cyclooxygenases (COX-1 and COX-2) [27] or upregulating negative regulatory signals, such as programmed cell death-1 (PD-1) ligands (PD-L1, PD-L2) and cytotoxic T lymphocyte antigen-4 (CTLA-4) [28–31]. We reported that PD-L1 expression in ovarian cancer is inversely correlated with tumor-infiltrating CD8+ T cells and is associated with a poor prognosis of the patient [20]. The expression of the immune suppressive factors COX and UL-16 binding protein 2 is also inversely associated with CD8+ T cell infiltration and the prognosis of the patient with ovarian cancer [21,32]. Thus, there are a variety of reports that suggest that a certain immunosuppressive factor influences the local tumor immunity. However, there are few comprehensive analyses that integrate various immune factors and evaluate the immune status as a whole.

Therefore, in this study, we attempted to explore the status of local immunity in ovarian cancers by integrating various immune parameters presented by the immunohistochemical analysis of clinical specimens. For this purpose, we employed bioinformatics analyses, such as hierarchical clustering, that allows the comprehensive assessment of multiple factors and enables us to determine the relationships among them.

2. Materials and Methods

2.1. Patients and Samples

Formalin-fixed, paraffin-embedded specimens were obtained from 70 patients who underwent primary surgery for epithelial ovarian cancer at the Kyoto University Hospital. After surgery, all patients received platinum- and paclitaxel-based chemotherapy. The average age of the patients was 55 years old (range, 26–78; standard deviation [SD], 11). At the end of the study, 29 (41%) patients had died from their disease, and 41 (59%) patients were alive. The mean follow-up period was 5 years (range, 0–11; SD, 3.0). All 70 tissue specimens were collected under the approval of the Ethics Committee of the Kyoto University Hospital.

2.2. Immunohistochemistry

The primary antibodies and antigen retrieval methods are listed in Supplementary Table 1. Briefly, formalin-fixed, paraffin-embedded specimens were cut into 4 μm-thick sections. The tissue sections were deparaffinized in xylene and dehydrated. For antigen retrieval for TGFβ1 and CD4 staining, the samples were boiled in Tris-EDTA buffer (pH 9.0) in a pressure cooker. For FOXP3 and PD-1 staining, the samples were boiled in citrate buffer (pH 6.0) in a pressure cooker. To block endogenous peroxidase activity, all of the sections were treated with 100% methanol containing H_2O_2. Nonspecific binding of IgG was blocked using normal rabbit serum (Nichirei, Tokyo, Japan). The sections were incubated with a mouse anti-TGFβ1 monoclonal antibody (Ab) (clone TB21), anti-CD4 monoclonal Ab (clone 1F6), anti-FOXP3 monoclonal Ab (clone 236A/E7) and PD-1 monoclonal Ab (clone NAT) overnight at 4 °C. Then the sections were incubated with biotinylated rabbit anti-mouse secondary Abs (Nichirei), followed by an incubation with a streptavidin–peroxidase complex solution. Signals were generated by incubation with 3, 3-diaminobenzidine. Finally, the sections were counterstained with hematoxylin and observed under a microscope.

2.3. Evaluation of the specimens

Immune cells in the intraepithelial space were counted using a microscopic field at 200× magnification (0.0625 mm^2). Five areas with the most abundant infiltration of immune cells were selected, and an average count was calculated. The result was interpreted as negative when fewer than five cells per 0.0625 mm^2 were observed and as positive when more than or equal to five cells were observed. The expression of TGFβ1 was evaluated according to the intensity of the staining and scored as follows: 0, negative; 1, very weak expression; 2, moderate expression; and 3, strongest expression. Cases with scores of 0 or 1 were defined as the low-expression group, and cases with scores of 2 or 3 were defined as the high-expression group. Two independent gynecological pathologists examined the immunohistochemical slides without any prior information regarding the clinical history of the patients.

2.4. Hierarchical clustering and statistics

Hierarchical clustering analysis of our immunohistochemical data was performed using the software Cluster 3.0 that was originally designed for manipulating cDNA microarray data [33]. Following the instructions of the software, the eleven parameters (six tumor-infiltrating immune cells and five immune suppressive factors) were normalized, and a complete-linkage hierarchical clustering was conducted. The dendrogram and heat map were graphically viewed using Java TreeView [33]. Cluster and Treeview software are freely available programs that can be accessed at http://jtreeview.sourceforge.net/.

2.5. Statistical analysis

Fisher's exact test and the χ^2 test were used to analyze the associations between each cluster and various clinicpathological factors. Spearman's correlation coefficient test was employed to analyze the associations among 11 immunological factors. Univariate analysis for overall survival was performed and evaluated with the log rank test, and Kaplan–Meier curves were generated. A multivariate Cox proportional-hazard model was used to evaluate the independency of Cluster 1 as a prognostic factor. Two-sided p values of <0.05 were considered to be significant.

3. Results

3.1. Expression of immune-suppressive factors in ovarian cancer specimens and patient prognosis

Immunohistochemical expression of TGFβ1, PD-L1, PD-L2, COX-1 and COX-2 was evaluated in 70 ovarian cancer tissues (Fig. 1). High expression (score 2 or 3) of TGFβ1 was observed in 22 cases (31.4%) and low expression (scored 0 or 1) was observed in 48 cases (68.6%). There was no correlation between the expression of these factors and clinicopathological characteristics such as age, histological type, FIGO stage, TNM classification, and residual tumor state (Supplementary Table 2) [20,32].

The log rank test showed that the 5-year survival rate of patients with high expression of TGFβ1, COX-1 or COX-2 was not significantly different from the patients with low expression (Supplementary Fig. 1). Only the high expression of PD-L1 was an independent worse prognostic factor, whereas PD-L2 expression was not related to patient prognosis [20].

The log rank test showed that the 5-year survival rate of patients with high expression of TGFβ1, COX-1 or COX-2 was not significantly different from the patients with low expression (Supplementary Fig. 1). Only the high expression of PD-L1 was an independent worse prognostic factor, whereas PD-L2 expression was not related to patient prognosis [20].

3.2. Tumor-infiltrating immune cell count and prognosis

The number of tumor-infiltrating CD1α+ (dendritic cells), CD4+ (helper T cells), CD8+ (killer T cells), CD57+ (NK cells), FOXP3+ (regulatory T cells) and PD-1+ immune cells was evaluated using the same 70 ovarian cancer specimens (Fig. 1). The average numbers of these cells were shown in Supplementary Table 3, respectively. There was positive correlation between tumor-infiltrating FOXP3+ cells and several clinicopathological factors such as age, histology, tumor status and residual tumor, while there was no correlation between the number of CD4+, CD8+, CD57+ or PD-1+ cells and clinicopathological characteristics (Supplementary Tables 4 and 5).

A significant correlation was found between parameters below; CD4+ cell infiltration vs. CD8+ cell infiltration, COX-1 and COX-2 expression, CD4+ cell vs. PD-1+ cell infiltration, CD8+ cell vs. PD-1+ cell infiltration, CD57+ cell vs. PD-1+ cell infiltration, FOXP3 cell infiltration vs. PD-L2 expression and FOXP3 vs. CD4+ cell infiltration (Supplementary Table 6), although a negative correlation between COX-1 vs. COX-2 expression, CD8+ cell infiltration vs. PD-L1 expression, CD8+ cell infiltration vs. COX-1 expression and CD8+ cell infiltration vs. COX-2 expression [20,32].

The log rank test showed that the overall survival rate of patients with high levels of CD1α+, CD4+, CD57+, FOXP3+ or PD-1+ immune cells was not significantly different from patients with low infiltration (Supplementary Fig. 1), whereas a high infiltration of CD8+ cells was the only beneficial prognostic factor ($p<0.001$) [20]. Combination of any two factors such as CD8+ and PD-L1 low did not serve as a superior prognostic factor compared with single factor. Besides we found a higher ratio of CD8/FOXP3 in Cluster 1 than that in Cluster 2–4, although there was no statistic significance (mean±SD, Cluster 1, 3.4±2.4 vs. Cluster 2–4, 1.9±1.9).

The log rank test showed that the overall survival rate of patients with high levels of CD1α+, CD4+, CD57+, FOXP3+ or PD-1+ immune cells was not significantly different from patients with low infiltration (Supplementary Fig. 1), whereas a high infiltration of CD8+ cells was the only beneficial prognostic factor ($p<0.001$) [20]. Combination of any two factors such as CD8+ and PD-L1 low did not serve as a superior prognostic factor compared with single factor. Besides we found a higher ratio of CD8/FOXP3 in Cluster 1 than that in Cluster 2–4, although there was no statistic significance (mean±SD, Cluster 1, 3.4±2.4 vs. Cluster 2–4, 1.9±1.9).

3.3. The correlation among eleven immunological factors

The correlation among eleven immunological factors (the expression of PD-L1, PD-L2, COX-1, COX-2 and TGFβ1 and the number of tumor-infiltrating immune cells expressing CD1α+, CD4+, CD8+, CD57+, FOXP3+ and PD-1+) was examined (Supplementary Table 6). The expression of PD-L1 or COX expression was negatively correlated with the number of CD8+ cells in the tumor site, respectively [20,32]. In this study, we found that the number of CD4+ cells was

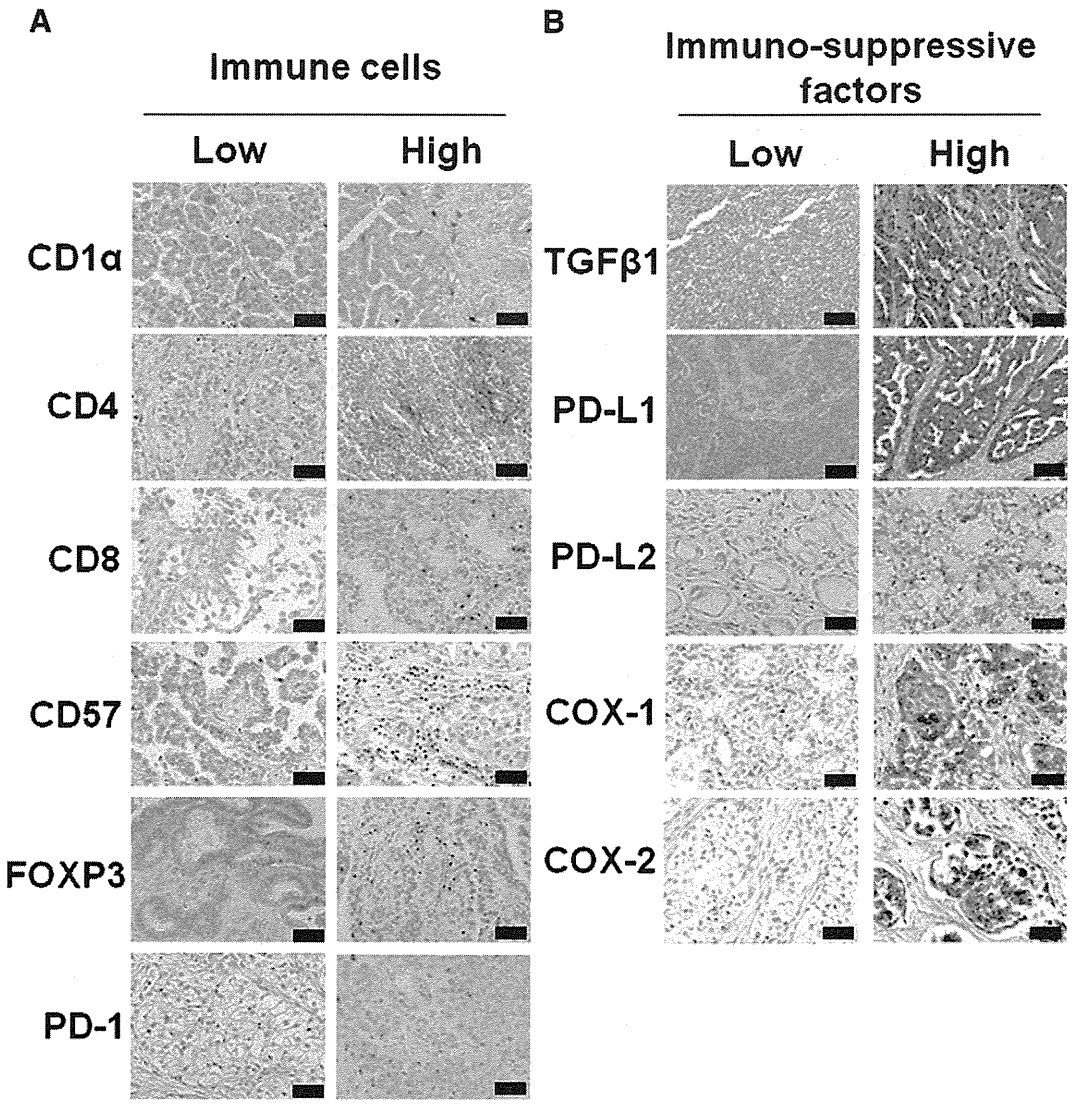

Figure 1 Immunohistochemical staining of human ovarian cancer tissue. (A) Representative staining patterns of ovarian cancers with low expression or with high expression of immunosuppressive factors, such as TGFβ1, PD-L1, PD-L2, COX-1, and COX-2, are shown. (B) Representative staining patterns with low or high infiltrating immune cells, such as CD1α+, CD4+, CD8+, CD57+, FOXP3+ or PD-1+ cells, in the tumor site are shown. Original magnification; (A and B) ×200. White bar, 200 μm.

positively correlated with the number of CD8+ cells (correlation coefficient ($R=0.240$; $p=0.045$) and FOXP3+ cells ($R=0.410$; $p<0.001$)). In addition, the number of PD-1+ cells showed a positive correlation with the number of CD4+ cells ($R=0.302$; $p=0.011$), CD8+ cells ($R=0.366$; $p=0.002$) and CD57+ cells ($R=0.365$; $p=0.002$). The number of FOXP3+ cells was negatively correlated with PD-L2 expression ($R=-0.262$; $p=0.028$).

3.4. Evaluation of the local immune status by hierarchical clustering of immune factors in ovarian cancer

Hierarchical clustering analysis of the expression levels of five immune suppressive factors and the cell counts of the six tumor-infiltrating immune cells were used to divide the 70 ovarian cancers into 2 major clusters and subdivided one of the major clusters into three clusters, which were designated as Cluster 1 and Clusters 2, 3 and 4, respectively (Fig. 2). When Cluster 1 was compared to the other clusters (Clusters 2–4), it was characterized as having significantly higher immune cell infiltration, such as CD4+ cells ($p=0.004$), CD8+ cells ($p<0.0001$) and PD-1+ cells ($p=0.0037$), and as having lower expression of immunosuppressive factors such as TGFβ1, PD-L1, PD-L2, COX-1 and COX-2 (Figs. 3A–C, F and 4).

The characteristics of the other three clusters were relatively common in terms of low immune cell infiltration and partially high expression of immune suppressive factors with the following patterns: Cluster 2, high COX-1 expression ($p<0.0001$) and high CD57+ cell (NK cell) infiltration ($p=0.0042$); Cluster 3, high PD-L2 ($p=0.0002$), low FOXP3+ cells ($p=0.0288$) and low PD-1+ cell infiltration ($p=0.011$); and Cluster 4, low CD4+, low CD8+, low CD1α+, low CD57+,

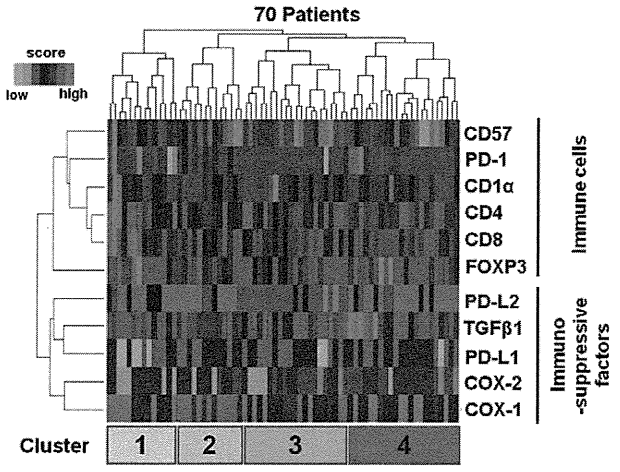

Figure 2 Graphic representation of the immune status of 70 ovarian cancer tissues. Patterns of immune status were classified into four clusters by hierarchical clustering based on six phenotype of immune cells, such as CD1α+, CD4+, CD8+, CD57+, FOXP3+ or PD-1+ cells, in the tumor site and five immunosuppressive factors, such as TGFβ1, PD-L1, PD-L2, COX-1 and COX-2. Separated clusters are indicated by dendrograms. The color bar indicates that red is the high score (expression or infiltration), while green is the low score.

low PD-1, high PD-L1, high TGFβ1, and high COX-2 (Figs. 3 and 4).

3.5. Univariate analysis and correlation between four clusters and clinicopathological factors

The Kaplan–Meier curve and log rank test showed that the overall survival rate of patients in Cluster 1 was significantly better than those in the other clusters (5-year survival rate in Cluster 1 vs. Clusters 2–4, 84.6% vs. 55.2%; $p=0.041$) (Fig. 5 and Table 1). The progression-free survival rate of patients in Cluster 1 was not significantly, but was relatively, better than other clusters (5-year survival rate of Cluster 1 vs. Clusters 2–4, 78.6% vs. 44.4%; $p=0.061$).

There was no statistical correlation between the four clusters and the clinicopathological factors such as primary tumor status, lymph node metastasis, distant metastasis, residual tumor status, the age of the patient, histology, and adjuvant chemotherapy (Table 2).

3.6. Multivariate analysis

Multivariate analysis showed that Cluster 1 was an independent favorable prognostic factor for overall survival (RR, 4.93) (Table 1). Other factors contributing to overall poor survival were tumor status (RR, 5.36), lymph node metastasis (RR, 2.78), and residual tumor status (RR, 5.86) (Table 1).

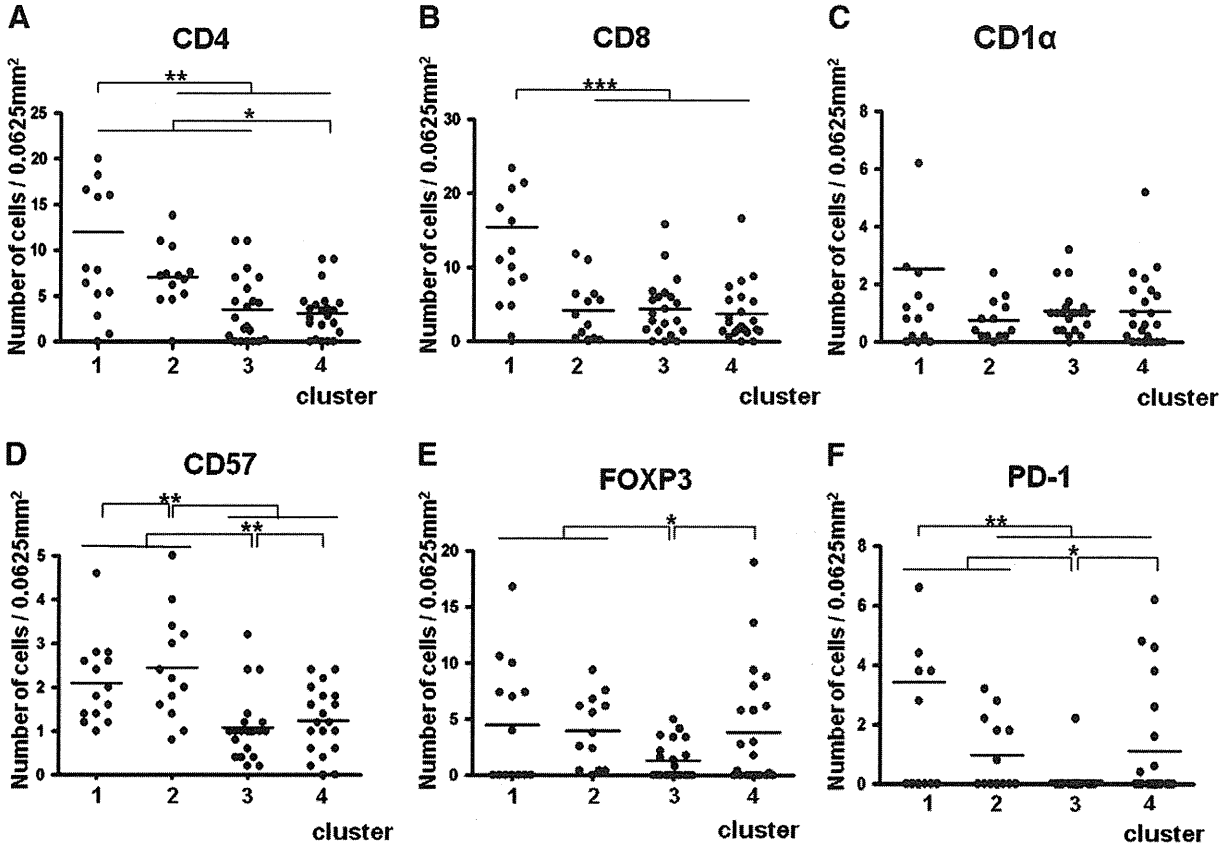

Figure 3 The patterns of immune cell infiltration into tumor sites in each cluster. The dot plots represent the number of immune cells in the four clusters; (A) CD4; (B) CD8; (C) CD1α; (D) CD57; (E) FOXP3; and (F) PD-1 (*$p<0.05$, **$p<0.01$, ***$p<0.0001$).

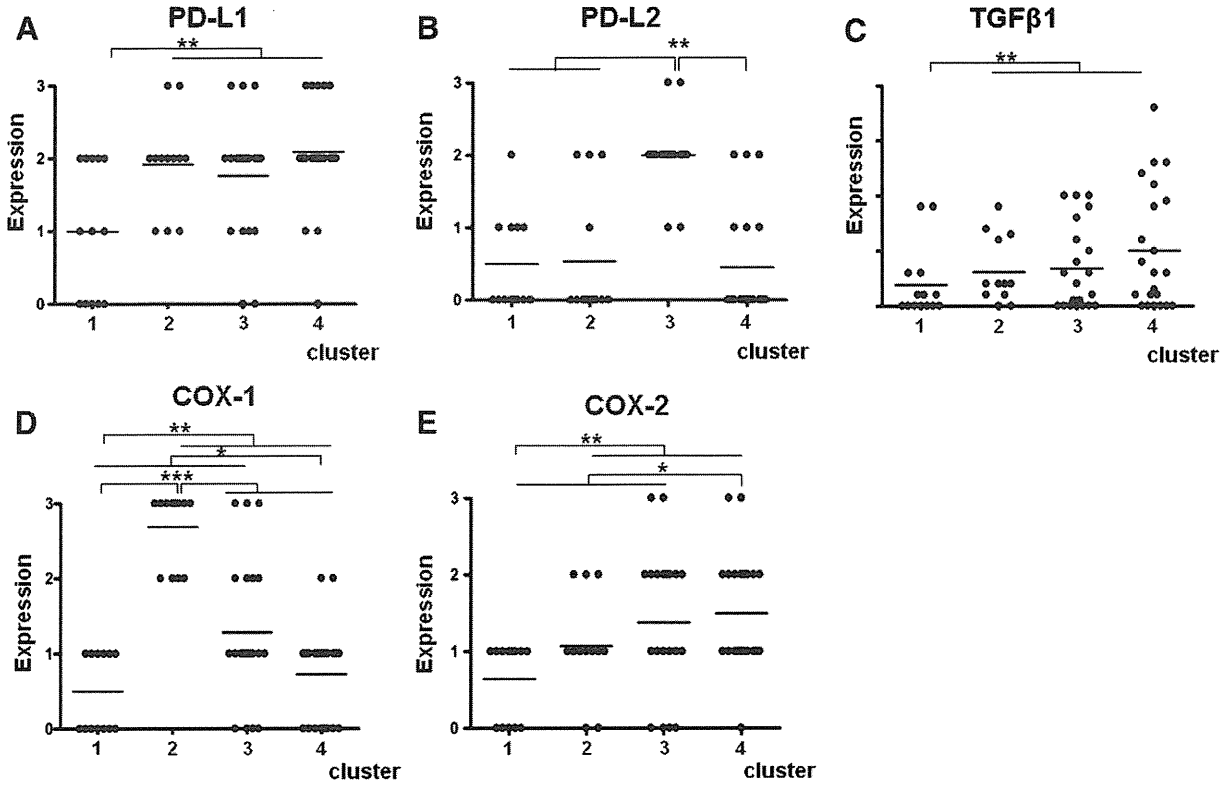

Figure 4 The patterns of immunosuppressive factor expression in each cluster. The dot plots represent the expression levels of immunosuppressive factors in the four clusters; (A) PD-L1; (B) PD-L2; (C) TGFβ1; (D) COX-1; and (E) COX-2 (*p<0.05, **p<0.01, ***p<0.0001).

4. Discussion

Recent studies have shown that local tumor immunity is closely associated with clinical course of cancer patient, and several immunological factors, including CD8 T cell count shown in our previous study, serve as prognostic indicator. However, these analyses were mainly done using single factor or combination of several factors, and there are few papers which tried to clarify the immunological background by analyzing multiple immune factors simultaneously. The application of hierarchical clustering allowed us to manage the complex data sets of immunohistochemical staining with multiple antibodies [34,35] and to identify new groups of patients with similar local immunological patterns that may be caused by similar consequences. Ovarian cancers were divided into two groups, Cluster 1 and Clusters 2–4, by hierarchical clustering analysis according to the local immunological state. The patients in Cluster 1 had a significantly better prognosis than those in other clusters (p=0.041, Fig. 5B). In this group, immune cells, including CD4+ cells, CD8+ cells and PD-1+ cells, were highly infiltrated into tumor sites compared to the other clusters (p=0.004, p<0.001 and p=0.0037, respectively), while the expression of TGFβ1, PD-L1, PD-L2, COX-1 and COX-2

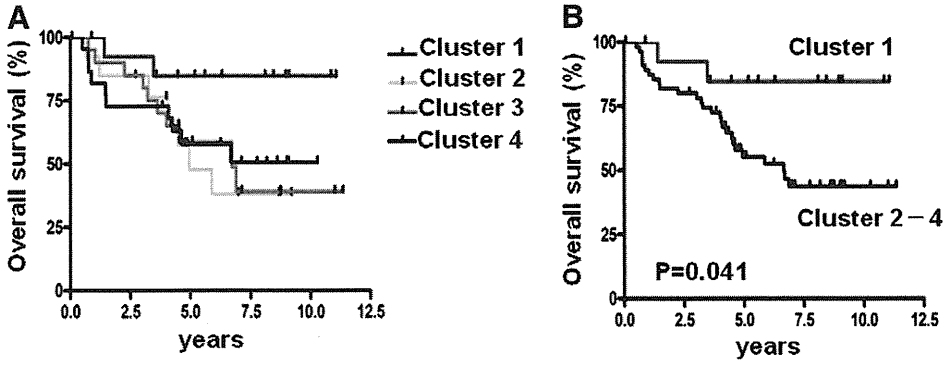

Figure 5 Overall survival analyses of patients with ovarian cancer according to the four clusters. (A) Kaplan–Meier curves according to Cluster 1 and the other clusters. (B) Kaplan–Meier curves according to Cluster 1 and the combination of other clusters.

Table 1 Univariate and multivariate analysis demonstrating the independent risk factors, including Cluster 1, on overall survival of patients with ovarian cancer ($n=70$).

	n	Overall survival			
		Univariate hazard ratio [a]	p	Multivariate hazard ratio [a]	p
Cluster			0.041		0.035
Cluster 1	38	1		1	
Clusters 2–4	32	3.98 (1.04–5.90)		4.93 (1.11–21.76)	
Tumor status			<0.001		0.013
pT1+pT2	31	1		1	
pT3	39	7.90 (2.73–22.83)		5.36 (1.42–20.20)	
LN metastasis			0.003		0.041
pN0	56	1		1	
pN1	14	3.24 (1.50–7.00)		2.78 (1.04–7.38)	
Distant metastasis			0.047		0.122
pM0	57	1		1	
pM1	13	2.28 (1.01–5.16)		2.44 (0.79–7.58)	
Residual tumor			<0.001		0.001
Optimal	49	1		1	
Suboptimal	21	4.54 (2.17–9.50)		5.86 (1.98–17.34)	
Histology			0.477		0.103
Serous type	33	1.33 (0.59–3.02)		3.27 (1.20–8.93)	
Non-serous type	37	1		1	
Chemotherapy			0.122		0.936
Paclitaxel	31	1		1	
No paclitaxel	39	1.79 (0.86–3.77)		1.03 (0.48–2.23)	
Age			0.486		0.562
<55	32	1		1	
≥55	38	1. 31(0.62–2.77)		1.268 (0.57–2.83)	

[a] The numbers in parenthesis represent the 95% confidence interval (C.I.).

were significantly low. In this group, PD-1+ cells may represent T cells in the late active phase [36], though its significance is to be clarified. Thus, Cluster 1 was characterized by high immune cell infiltration and low expression of all immunosuppressive factors studied (Figs. 3 and 4), suggesting that host-tumor immunity in the tumor microenvironment is still maintained in this group, which may lead to the significantly better prognosis. Besides a ratio of CD8/FOXP3ratio in Cluster 1 was higher than that in Cluster 2–4, although there was no statistic significance, which is a similar tendency to the previously published report [19].

Clusters 2–4 were characterized by a low level of immune cell infiltration and high expression of immunosuppressive factors and had significantly worse prognoses than Cluster 1. Cluster 2 was characterized by a significantly high expression of COX-1, whereas Cluster 3 and 4 had significantly high expressions of COX-2 ($p=0.0053$ and $p=0.0048$, respectively). The immunoregulatory function of COX-2-induced prostaglandin E2 (PGE_2) is known to be important in inducing immune tolerance in the tumor microenvironment [37]. Secreted from tumor cells, PGE_2 alters the Th1/Th2 balance, suppresses lymphocyte proliferation, and regulates the function of antigen presenting cells [37,38]. There is a report that expression of COX-2 is an independent prognostic factor in human ovarian carcinoma [39]. Hence, high expression of COX-2 in Cluster 3 and Cluster 4 may contribute to poorer prognosis associated with low CD8+ cell infiltration (Figs. 3–5 and Supplementary Table 6). Similarly, COX-1 expression was inversely correlated with CD8+ cell infiltration in Cluster 2, which may partly explain the poor prognosis of Cluster 2.

Cluster 3 was characterized by high PD-L2 expression and low PD-1+ cell infiltration and had a worse prognosis. We previously reported that the patient with high expression of PD-L2 had a tendency for poor prognosis, although the difference was not statistically significant. In this respect, high expression of PD-L2 may partly explain the poor prognosis of this group, possibly by negatively influencing the infiltration of CD8+, CD4+ and PD-1+ cells. Cluster 4 was characterized by high expression of PD-L1, TGFβ1 and COX2 and low CD8+ cell infiltration. Previous studies on PD-L1 expression in malignant tumors, such as in kidney, bladder, breast, gastric, pancreatic and ovarian cancer, have shown that PD-L1 has a negative impact on the survival of the patient [29]. In addition, PD-L1 expression was inversely correlated with intraepithelial infiltrating CD8+ T cells, suggesting that PD-L1 inhibits the intratumoral infiltration of CD8+ T cells. TGFβ signaling has been implicated in tumor progression, metastasis and immunosuppression in the advanced tumor phase [25]. These results suggest that PD-1 ligand and/or COX expression are associated with an unfavorable clinical outcome of the patient by influencing the local immune environment.

Recently, three phases of cancer immunoediting, namely, "elimination", "equilibrium" and "escape" [4,6,40], have been proposed. In the first "elimination" phase, innate and adaptive immune cells recognize and eliminate tumor cells by immunosurveillance, protecting the host against cancer. In the second "equilibrium" phase, ongoing tumor growth

Table 2 Correlations between the four clusters and clinicopathological characteristics in ovarian cancer (n=70).

	n	Cluster 1	Cluster 2	Cluster 3	Cluster 4	p
Age						0.922
<55	32	6	8	10	10	
≥55	38	8	5	11	12	
Stage						0.972
I	27	6	3	9	9	
II	4	1	0	1	2	
III	26	5	5	8	8	
IV	13	2	5	3	3	
Histology						0.672
Serous	33	7	9	8	9	
Clear cell	22	5	2	9	6	
Endometrioid	11	1	1	4	5	
Mucinous	2	0	0	0	2	
Others	2	1	1	0	0	
Tumor status						0.889
pT1+pT2	31	6	4	10	11	
pT3	39	8	9	11	11	
LN metastasis						0.566
Positive	14	2	5	4	3	
Negative	56	12	8	17	19	
Distant metastasis						0.499
Positive	13	2	5	3	3	
Negative	57	12	8	18	19	
Residual tumor						0.773
Optimal	49	10	7	16	16	
Suboptimal	21	4	6	5	6	
Chemotherapy						0.965
No paclitaxel	39	9	7	12	11	
Paclitaxel	31	5	6	9	11	

and immune surveillance enter into a dynamic balance with one another, yielding in a protracted period. In the last "escape" phase, the tumor avoids immune-mediated destruction and develops into a clinically apparent neoplasm [4]. This hypothesis is mainly applied to the process of cancer development in which immunosurveillance is gradually impaired. However, in clinical situations, cancer patients sometimes experience an asymptomatic period coexisting with known cancer lesions, or even a spontaneous regression, without any medical interventions, suggesting that the balance between tumor growth and host immunity significantly influences the clinical course of cancer patients. Nevertheless, there have been few studies that intended to comprehensively analyze the local immune status of each case, which would thereby establish the means to predict the clinical outcome. In this study, Cluster 1 may represent a phenotype of the "equilibrium" phase, where immune cells infiltrate into the tumor site to eliminate the tumor. Clusters 2, 3 and 4 may be in "escape" phase in which the local immune environment has already fallen into an immunosuppressive status. For an effective immune therapy, an understanding of the immune status in each case is particularly important. This study provides a model to analyze the complicated immune reaction in a local tumor site.

This study may also provide a future direction for order-made immunotherapy in each ovarian cancer patient. Currently, therapeutic modalities to target specific immunosuppressive factors are being developed. Blocking antibodies against PD-1 (MDX-1106) have been developed and are in Phase I clinical trials for advanced refractory malignancies [41]. Phase II and III clinical trials using selective COX2 inhibitors, celecoxib and rofecoxib, in combination with a chemotherapeutic have shown a clinical benefit [42]. Clinical trials focusing on the inhibition of the TGFβ signaling pathway by a monoclonal antibody or a small molecule inhibitor of the TGFβ receptor I kinase are being performed. To select the most efficient single or combined immune targeting therapies, precise assessments with multiple immune parameters in each case is essential.

In conclusion, hierarchical clustering of tumor-infiltrating immune cells and immunosuppressive factors was used to identify a subgroup of ovarian cancer patients with a better prognosis. This study also suggested that immunosuppressive factors might influence the pattern of tumor-infiltrating immune cells. The approach to comprehensively analyze multiple immune factors shown here may lead to a precise understanding of the local immune status and provide a tool for the application of immune therapies to treat ovarian cancer patients.

Supplementary materials related to this article can be found online at doi:10.1016/j.clim.2011.08.013.

Conflict of interest statement

The authors declare no conflict of interest.